https://doi.org/10.5194/essd-2021-176
Preprint. Discussion started: 11 June 2021

Open Access Earth System Science Data Discussions

Kinematic observations of the mountain cryosphere using in-situ GNSS instruments

Jan Beutel[1,2], Andreas Biri[2], Ben Buchli[2], Alessandro Cicoira[3,4], Reynald Delaloye[4], Reto Da Forno[2], Isabelle Gaertner-Roer[3], Stephan Gruber[5], Tonio Gsell[2], Andreas Hasler[6], Roman Lim[2], Philippe Limpach[7], Raphael Mayoraz[8], Matthias Meyer[2], Jeannette Noetzli[9], Marcia Phillips[9], Eric Pointner[10], Hugo Raetzo[11], Cristian Scapozza[12], Tazio Strozzi[13], Lothar Thiele[2], Andreas Vieli[3], Daniel Vonder Mühll[14], Samuel Weber[2,3,15], and Vanessa Wirz[3]

[1]Department of Computer Science, University of Innsbruck, Austria
[2]Computer Engineering and Networks Laboratory, ETH Zurich, Switzerland
[3]Department of Geography, University of Zurich, Switzerland
[4]Department of Geosciences, University of Fribourg, Switzerland
[5]Carleton University, Ottawa, Canada
[6]SensAlpin GmbH, Davos, Switzerland
[7]Terradata AG, Zurich, Switzerland
[8]Ct. Valais, Sion, Switzerland
[9]WSL Institute for Snow and Avalanche Research SLF, Davos, Switzerland
[10]Rovina und Partner AG, Visp, Switzerland
[11]Federal Office for the Environment FOEN, Ittigen, Switzerland
[12]Institute of Earth Sciences, University of Applied Sciences and Arts of Southern Switzerland (SUPSI), Switzerland
[13]GAMMA Remote Sensing and Consulting AG, Gümlingen, Switzerland
[14]Personalized Health and Related Technologies, ETH Zurich, Switzerland
[15]Chair of Landslide Research, Technical University of Munich, Germany

Correspondence: Jan Beutel (jan.beutel@uibk.ac.at)

Abstract. Permafrost warming is coinciding with accelerated mass movements, talking place especially in steep, mountainous topography. While this observation is backed up by evidence and analysis of both remote sensing as well as repeat terrestrial surveys undertaken since decades much knowledge is to be gained about the specific details, the variability and the processes governing these mass movements in the mountain cryosphere. This dataset collates data of continuously acquired kinematic observations obtained through in-situ Global Navigation Satellite Systems (GNSS) instruments that have been designed and implemented in a large-scale multi field-site monitoring campaign across the whole Swiss Alps. The landforms covered include rock glaciers, high-alpine steep bedrock bedrock as well as landslide sites, most of which are situated in permafrost areas. The dataset was acquired at 54 different stations situated at locations from 2304 to 4003 m a.s.l and comprises 209'948 daily positions derived through double-differential GNSS post-processing. Apart from these, the dataset contains down-sampled and cleaned time series of weather station and inclinometer data as well as the full set of GNSS observables in RINEX format. Furthermore the dataset is accompanied by tools for processing and data management in order to facilitate reuse, open alternate usage opportunities and support the life-long living data process with updates. To date this dataset has seen numerous use cases in research as well as natural-hazard mitigation and adaptation due to climate change.

https://doi.org/10.5194/essd-2021-176
Preprint. Discussion started: 11 June 2021

Open Access Earth System Science Data Discussions

1 Introduction

The detailed observation of mass movements with the help of in-situ Global Navigation Satellite Systems (GNSS) instruments across different scales has been intensively investigated over the past decade (Wirz et al., 2013; Ravanel and Deline, 2014; Kenner et al., 2020; Cicoira et al., 2019b). The advantage of this method for assessing surface displacements over traditional field-surveying methods or remote sensing techniques is the unprecedented level of detail that can be obtained w.r.t. these surface movements. Today it is possible to monitor at millimeter scale with a temporal resolutions of minutes using commodity receiver hardware similar to those found in consumer products, e.g. mobile phones or automotive systems (Paziewski et al., 2021) using double differential GNSS processing techniques (Teunissen and Montenbruck, 2017) with a cost footprint several orders of magnitude lower than required for traditional geodetic surveying equipment (Wirz et al., 2013). Depending on the fidelity required the accuracy and temporal resolution is achieved by operating GNSS receiver pairs continuously and post-processing the observation data. This typically results in a large energy and data footprint required but equally it has been shown that by selectively duty-cycling receivers and transmitting the GNSS observation data on a low-power wireless sensor network (Buchli et al., 2012) tradeoffs between energy/data volumes required and the fidelity achieved can be made. This now allows permanent monitoring in near real-time in the most remote locations. The success of the method is clearly demonstrated by the scaling out to multiple stakeholders and applications of this methodology and the instruments developed in the initial project as documented in this paper. This is especially visible by the fact that in 2019, the Swiss Permafrost Monitoring Network PERMOS has adopted the method of permanently installed GNSS systems as a further monitoring element into it's portfolio to systematically documents the state and changes of mountain permafrost in the Swiss Alps, an integral part of the Global Terrestrial Network for Permafrost (GTN-P) established within the worldwide climate-monitoring program (GCOS/GTOS).

In this paper we document a unique data set of kinematic observations of the mountain cryosphere obtained in the Swiss Alps over the past decade using in-situ GNSS instruments at high altitude. We publish the coordinate series of 54 GNSS measurement positions obtained by double-differential GNSS post-processing, including in-situ inclinometer and accompanying weather station data, as well as the raw GNSS observables of all GNSS station. The data covers sites of different landforms and morphologies spread out all over Switzerland: rock glaciers, high-alpine landslides, single bedrock features/blocks as well as small and large rockfall sites. The elevation of the 54 observation points ranges from 2304 to $4003\,\mathrm{m}$ a.s.l.. The data set contains the complete raw data at full sampling rates of all instruments used (the primary data set; see Sect. 4) as well as a selection of derived data products (the secondary data set, see Sect. 5). The derived data products are down-sampled and cleaned time series of weather station and inclinometer data as well as GNSS daily positions computed using double differencing techniques. The raw GNSS observables data will enable to develop further improved processing methods, atmospheric (Hurter et al., 2012) and ground-based (Henkel et al., 2018) observations, or educational purposes.

A toolset (Weber et al., 2019b) originally created for (Weber et al., 2019a) allows to (re-)create and independently update (living data process) the data documented in this paper[1]. This toolset is an update of the toolset created for the companion data paper describing the Matterhorn Hörnligrat field site (Weber et al., 2019a). For a more detailed description of the wireless

[1] Available at https://gitlab.ethz.ch/tec/public/permasense/permasense_datamgr.

https://doi.org/10.5194/essd-2021-176
Preprint. Discussion started: 11 June 2021

Open Access Earth System Science Data Discussions

technology used in this paper, the data management infrastructure and the joint online data portal at http://data.permasense.ch we refer to the original publication (Weber et al., 2019a).

Figure 1. Two GNSS sensing devices mounted atop large boulders found on the landforms being monitored. Breithorn Landslide 2982 m a.s.l., Herbriggen (Switzerland) (left); Largario rock glacier 2355 m a.s.l., Blenio (Switzerland) (right). © PermaSense Project

In addition to compiling and documenting the data set, selected examples of past work as well as an overview of the scientific results based on this data set are discussed in Sec. 6. In the following section 2, we present a brief history of the project and a description of the instrumented field sites with a focus on past activities and natural hazard history. Section 3 describes the technical measurement system and instruments used.

2 Field sites and project history

The X-Sense project (Beutel et al., 2011) was a large interdisciplinary research project targeting to detect and analyze the temporal and spatial variability of high-alpine slope movements with the help of permanently installed custom-designed low-cost GNSS sensors. The X-Sense project, conducted from 2010 to 2013, focused on a study area on the orographic right side of the Matter Valley above the municipalities of Randa and Herbriggen (Switzerland), where numerous slope movements endanger the livelihood in the areas on the valley floor. The area is dominantly situated in permafrost and is very feature rich (Wirz et al., 2013), see Fig. 2. Specifically there exist active and relict rock-glaciers, landslides, solifluction lobes, fractures, sackung etc. (Delaloye et al., 2013; Wirz et al., 2014b). The method devised in this initial project (Buchli et al., 2012; Wirz et al., 2013) has proven very successful and was thus expanded to other locations and applications of monitoring (Kenner et al., 2018; Cicoira et al., 2021) as well as natural hazard mitigation (Kenner et al., 2020) in collaboration with partners of the Swiss Permafrost Monitoring Network (PERMOS), the Swiss cantonal and federal authorities (Randa Grossgufer, Wysse Schije, PERMOS GNSS sites) (Noetzli et al., 2019). The methodological approach and technology used is closely related to work that was pioneered at the Matterhorn Hörnligrat field site from 2008 (Talzi et al., 2007; Hasler et al., 2008) as well as the

https://doi.org/10.5194/essd-2021-176
Preprint. Discussion started: 11 June 2021

Open Access Earth System Science Data Discussions

Jungfraujoch (Hasler et al., 2011). For the sake of completeness the GNSS data already published in (Weber et al., 2019a) for the Matterhorn Hörnligrat is included in this publication as well.

Figure 2. The Grabengufer rock glacier is issuing significant material during a surge period in winter 2009 is fed from a landslide in the snowy depression above where 5x GNSS locations are present, Randa (Switzerland) (left). A GNSS sensor monitoring the terrain movement in the area of Längschnee 2588 m a.s.l. above the village of Herbriggen (Switzerland) (right). © PermaSense Project

Apart from obtaining sensor data and working on geoscientific process studies, this project also focused on developing and proving the utility of low-power wireless GNSS sensing system in the scope of the application described. As mentioned earlier a new set of sensors was developed based on commodity L1-GPS receivers and ubiquitous wireless data access based on previous work on the Matterhorn (Hasler et al., 2008, 2012; Weber et al., 2017) and Jungfraujoch (Hasler et al., 2011; Girard et al., 2012) (see Sect. 3).

The main challenge apart from designing a robust and long-lived sensing system suitable for year-around operation in an high-alpine setting lies in the fact that the GNSS sensors employed are characterized by (i) large data volumes and (ii) a significant power consumption compared to many other in-situ sensors used in this domain. This has its cause in the fact that in order to obtain sufficient observation data from the satellite constellation both w.r.t. quality and quantity the GNSS receiver needs to be operated continuously over large periods of time (typically hours) and without using any low-power operating modes and also using an active antenna. For the resolution of very small displacements, such as in compact bedrock or the ability to react fast on changing displacement dynamics, e.g. in natural hazard scenarios a 24/7 operation of the sensors is required. The resulting energy and data footprint of the GNSS sensor alone (without data logging and data transmission) is on the order of Watts and Megabytes per station and per day significantly exceeding typical requirements of geoscientific data acquisition systems, e.g. a typical data logger with sensors attached.

2.1 Deployment context and evolution

The deployment activities of GNSS sensors started in summer 2010 on the central orographic right side of the Matter Valley near the Dirruhorn rock glacier above the village of Herbriggen. Starting from there the newly developed GNSS sensors were

https://doi.org/10.5194/essd-2021-176
Preprint. Discussion started: 11 June 2021

Open Access Earth System Science Data Discussions

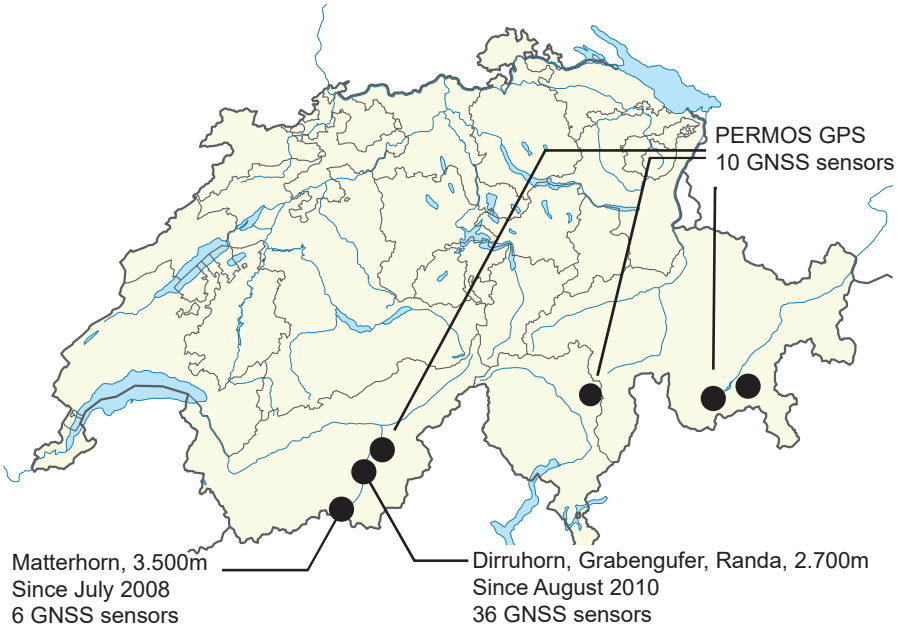

Figure 3. The field sites described in this paper are scattered throughout the high alpine areas of Switzerland.

tested and put to use to survey kinematics across different landforms and hazard areas (Wirz et al., 2014b). Further extensions took place to the Steintälli rock glacier, the Gugla/Bielzug rock glacier, the Längschnee, Breithorn, Gugla landslide areas as well as the Grabengufer above Randa. This area has a rich history w.r.t. mass movement-related natural hazards. Specifically, the earliest known records for hazards mitigation efforts date back to 1945 (subsidies by the Swiss federal government for rock wall protection measures near the Grabengufer) and February 1959 (evacuation of the village of Herbriggen due to an excessive landslide spontaneously developing on the Längschnee/Gugla area). During the study period further hazard and mitigation events took place where the data documented by and supplementing this paper served as integral component for decision making by the Swiss cantonal and federal authorities. A selection of the most noteworthy events and measures are described in the following: In spring 2013 excessive discharge from the Gugla/Bielzug rock glacier causes severe debris flow in the Bielzug torrent causing a partial evacuation of the village of Herbriggen. Subsequently a new catchment, dam as well as geophone-based monitoring was projected and erected. In order to protect hikers crossing the Grabengufer a hanging bridge spanning the upper part of the discharge gully (see Figure 2 left) was constructed in 2010. Due to the rapid evolution of the Grabengufer rock glacier and feeding landslide above in that time, the bridge was hit multiple times by debris discharged, subsequently closed and dismantled. In 2017 a new bridge with a span of $494\,\mathrm{m}$ a.s.l. was erected further downslope in the gully. In 2018, a large boulder on the order of $2000\,\mathrm{m}^3$ was blasted in a two-month effort to protect the village of Randa below (see Figure 4). This freestanding boulder was located at the fringe of the landslide feeding into the Grabengufer rock glacier and was gradually revealed due to continuous erosion happening due to the excessive slope movements in the area. In the area of Längschnee a large rock boulder ($2524\,\mathrm{meter}$ a.s.l.) was stabilized with pylon anchors and concrete underfilling in 2014.

https://doi.org/10.5194/essd-2021-176
Preprint. Discussion started: 11 June 2021

Here, the monitoring of slope movement using 3x GPS on instable masses and 1x GNSS sensor on the stabilized rock serve as integral part of the protection measures for the village of Herbriggen. Due to the recent evolution, this village has received a new hazard zonation in 2018 and recently four large protective dams have been erected on the upper limit of the village. In the Ritigraben area, the rock glacier has repeatedly led to severe debris flow with impact on the road, railway track and Matter Vispa river below. The most notable event was in 2018 when the debris discharged by the Ritigraben rock glacier blocked up the river and caused severe flooding all the way into the central sewage treatment plant of the valley (Kenner et al., 2017, 2018).

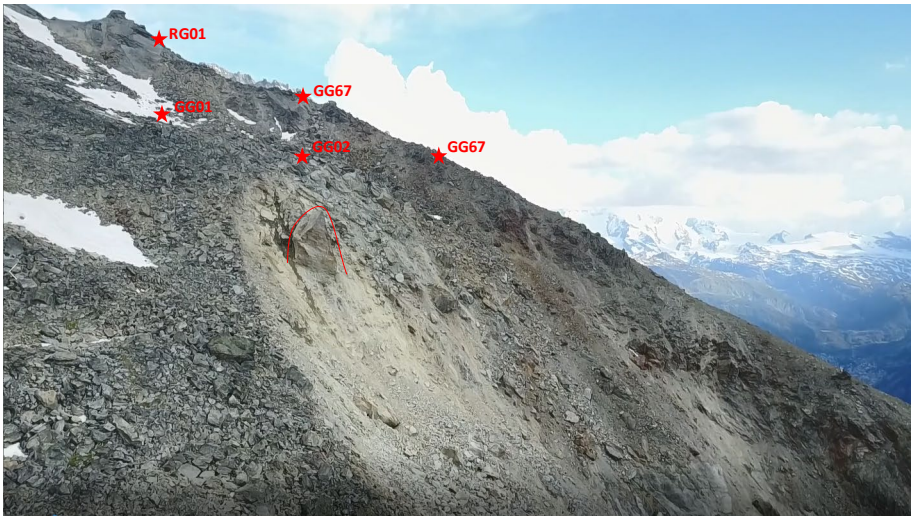

Figure 4. The freestanding boulder of approximately $2000\,\mathrm{m}^3$ was blasted as a precautionary measure in 2018. Above the boulder several GNSS monitoring positions are marked that are located in and around the landslide zone feeding the Grabengufer rock glacier below. © PermaSense Project

The Grossgufer above Randa is one of the most prominent and largest rockfall sites in the Alps with a size of approx. $30 \times 10^6\,\mathrm{m}^3$ (Willenberg et al., 2008b, a). In a joint activity with national and regional authorities as well as a local engineering firm a monitoring concept with in-situ GNSS sensors was implemented along the upper crest of the rockfall fault line. Additionally the infrastructure built for the hazard mitigation and monitoring of this 1991 rockfall site serves as a host site for wireless network infrastructure (see Sec. 3) and as a local geodetic reference that is situated on solid bedrock above the actual rockfall. Also situated on the orographic left side of the valley and close to the Grossgufer is the site of the Wysse Schije that features extensive rockfall protection measures above a series of of avalanche protection structures. Here a single GNSS sensor is monitoring the pronounced slope movement for monitoring and mitigation purposes as well.

Further rock glaciers in the Matter and Saas Valley have been instrumented as well: The Distelhorn rock glacier is situated to the north above the village of Grächen and the Gruben (Haeberli, 1996) and Jäggihorn rock glaciers are situated on the orographic right side of the Saas valley above the village of Saas Grund. All of these pose a significant hazard potential that is either historically been investigated of is of immediate current interest.

https://doi.org/10.5194/essd-2021-176
Preprint. Discussion started: 11 June 2021

The success of this in-situ kinematic monitoring methods and instrumentation developed in the context of the X-Sense project is further manifested by the fact that this technology has been chosen to also monitor sites with similar properties as the above mentioned in other regions of Switzerland. The Schafberg (Kenner et al., 2020), Muragl (Kääb et al., 1997; Kaeaeb et al., 1998), and Murtel-Corvatsch rock glaciers (Cicoira et al., 2019a, 2021) are situated in the Upper Engadin valley and the Largario rock glacier is situated in the Blenio valley, TI (Scapozza et al., 2014).

2.2 Key observations, trends and significance of the dataset

The X-Sense project has been almost entirely developed within the periglacial environment, strongly affected by permafrost and its recent evolution, characterized by a continuous warming of permafrost temperatures and increasing displacement rates in the affected landforms (Biskaborn et al., 2019; Noetzli et al., 2019) (See Fig. 5). Kinematic monitoring activities in this environment are notably more challenging than in others environments (e.g. in the glacial realm) due to their invisible nature, often characterized by small movements (Arenson et al., 2016). Prior to this project, geodetic surveys were the main method of investigation, with many advantages but also some major limitations to the number of survey points, the amount of personnel involved and the specifically the temporal resolution. Based on the in-situ sensor technology described in this paper (Buchli et al., 2012), the pioneering work of Vanessa Wirz (Wirz et al., 2013, 2014b) followed by detailed studies on the processes controlling rock glacier movement and their drivers (Cicoira et al., 2019a, b) brought about a paradigm shift in rock glacier research. In fact, these studies investigated for the first time sub-seasonal variations in permafrost-affected landslides and rock glaciers and combined them to long-term trends observed here and from other monitoring programs (Noetzli et al., 2019). The combination of kinematic and meteorological data allowed to extend the analysis to dynamics, highlighting the importance of hydrological processes in the evolution of the alpine periglacial environment.

In recent years, drone-based photogrammetry, laser scanning and remote sensing techniques, specifically the application of terrestrial as well as satellite-based InSAR have largely advanced the field by providing dense point clouds of large areas enabling analysis over different periods of time to create velocity fields and historical time-series (Kääb et al., 2021; Strozzi et al., 2020; Marcer et al., 2021). But of course, these approaches need ground truth data for validation and for scaling and this is where the fine-grained continuous kinematic measurements using stationary GNSS sensors factor in. In this sense, the GNSS data presented in this manuscript proves to be an indispensable tool for the quantitative assessment of the accuracy of remote sensing approaches as well as a still unique dataset with regard to the temporal resolution for detailed process- and climate-oriented studies. These advances are leading the way, in combination with ongoing efforts to create standardised methodologies for rock glacier inventorying, towards creating a global monitoring strategy and universal data products to allow the investigation of permafrost kinematics in the context of an Essential Climate Variable (ECV) associated to the Global Climate Observing System (GCOS) (Delaloye et al., 2018).

Due to the demonstrated reliability of the instruments and data, the expressiveness of near real-time kinematics and the capability to scale scales we have demonstrated the utility of the method of in-situ GNSS sensors for the mitigation of natural hazard scenarios and adaptation to climate change. Specifically the technology transfer from research prototype methodology to multiple public stakeholders like local communities, regional as well as federal government as well as the adoption as a new

https://doi.org/10.5194/essd-2021-176
Preprint. Discussion started: 11 June 2021

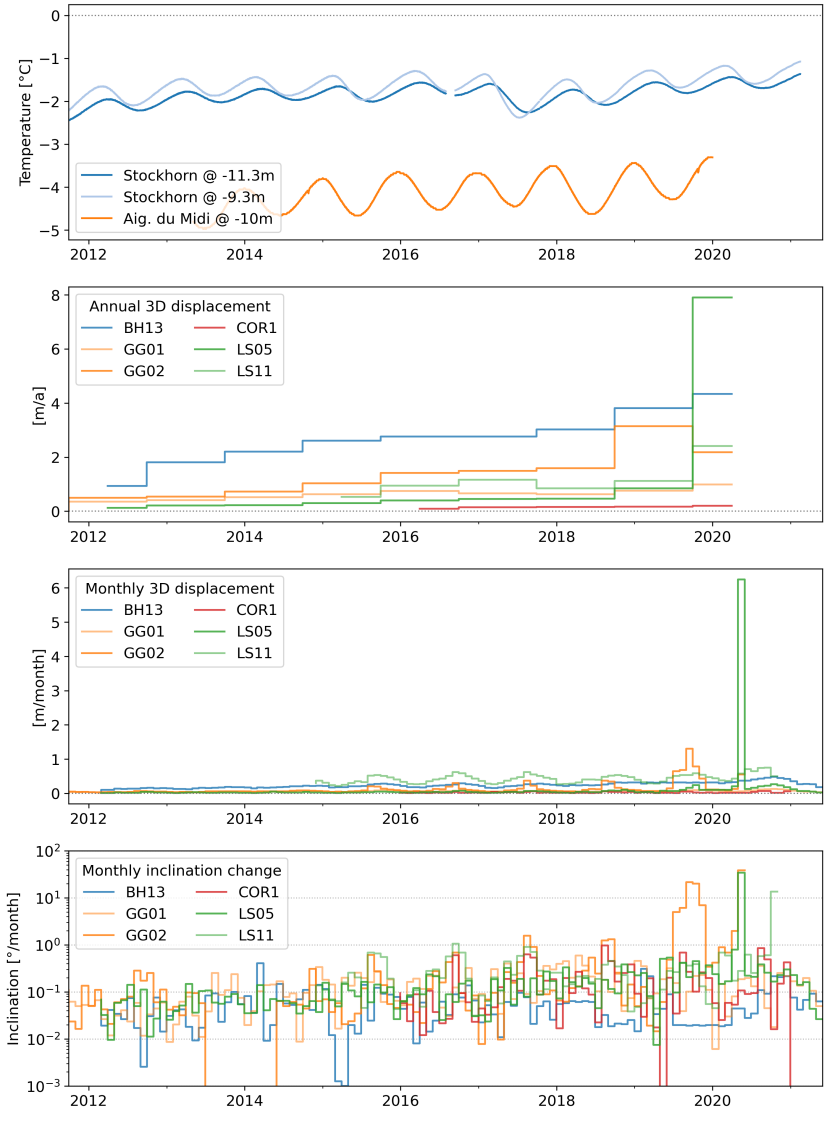

Figure 5. Accelerating trends observed in cryosphere related slope movements coincide with warming trends observed in permafrost boreholes. Here, selected slope movements from three rock glaciers (BH13, COR1, GG01, GG02) and a landslide in permafrost terrain (LS05, LS11) are shown with annual displacements per hydrological year as well as monthly displacements and monthly aggregate inclination changes observed. The data of LS05 shows a large slip displacement in the year 2020.

https://doi.org/10.5194/essd-2021-176
Preprint. Discussion started: 11 June 2021

measurement segment within the national permafrost monitoring network (PERMOS) clearly show the impact of the results and data obtained. As such, the data and methodology documented in this data publication has become an integral part of the monitoring portfolio to systematically document the state and changes of mountain permafrost in the Swiss Alps, an integral part of the Global Terrestrial Network for Permafrost (GTN-P) established within the worldwide climate-monitoring program (GCOS/GTOS).

3 Technical measurement setup

The measurement setup consists of distributed GNSS instruments that are permanently installed on a location of interest, i.e. the surface of a land form under investigation. Each instrument consists of a GNSS receiver, a GNSS antenna, a two-axis inclinometer, a data logger and in many cases a wireless transmission system. Typically the instrument is mounted on top of a rock outcrop or a boulder large enough for a stable positioning. In order to facilitate operation with extended snow cover in winter the instrument is mounted on top of a mast that keeps the GNSS antenna and solar panel above the snow cover for as much as possible. At select positions a non-moving location in the terrain has been equipped with a supplementary GNSS instrument acting as position reference for double-differential GNSS post-processing with a shorter baseline than when other GNSS infrastructure or the national reference network. Additionally these reference locations also act as a collection point for data collected using a Wireless Sensor Network (WSN) connecting all GNSS measurement points.

Power for all instruments is provided by standard photovoltaic systems: A solar panel, a charge controller and a 12V Absorbed Glass Mat (AGM) sealed lead-acid battery. The solar panel is typically mounted directly on the GPS mast (see Fig. 1, 11).

3.1 GNSS sensor instruments

The GNSS sensor instruments used are based on commodity GNSS receivers with the extended capability to output the raw satellite observables (u-blox LEA-6T) and an active antenna (Trimble Bullet III) (Wirz et al., 2013; Buchli et al., 2012). Furthermore a two-axis inclinometer (Murata SCA830), and ambient temperature/humidity sensor (Sensirion SHT31) and power supervisory circuits are also integrated. The first generation instruments we capable of logging data to internal SD-card storage only whereas later generations of devices are capable of data transmission in near-real time over a wireless network. In order to reduce the necessary power footprint, e.g. at times of reduced solar radiation for energy harvesting, a sampling schedule can be set on each device. This sampling schedule has hourly granularity and on-windows are typically centered at 12:00:00 UTC.

Starting with a proof-of-concept study in 2010, first a logging only GNSS sensor was developed (Wirz et al., 2013) that was subsequently refined into two wireless systems: One focused on experimentation (Beutel et al., 2011) and a final fully integrated production sensor system, the wireless GPS sensor (Buchli et al., 2012) (see Fig.6). This two-stop approach allowed for fast startup independent from infrastructure and network coverage. Over time, most of the sensor locations have been equipped with wireless data transmission greatly facilitating sensor operation and near realtime data retrieval (see Tables 16, 17).

https://doi.org/10.5194/essd-2021-176
Preprint. Discussion started: 11 June 2021

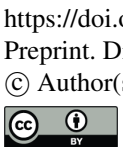

Open Access Earth System Science Data Discussions

Figure 6. Three generations of GNSS sensors have been developed: A GPS logger, an integrated wireless platform based on a Linux Single Board Computer and WLAN as well as a fully integrated Wireless GPS Sensor.

3.2 Inclination sensors

Two-axis inclinometers are integrated in the sensor systems to be able to correct the tilt of a mast, i.e. correct the translatory movement at the top vs. the base the mast (Wirz et al., 2013). Experience has shown that this correction can yield favorable results (Wirz et al., 2014a) but the exact point of rotation of the mounting point still remains unclear in most cases since the extent of the boulder below the earth surface is not known. However it has shown that the time series data derived from these inclinometers is very expressive proxy data for the movement of the location as can be seen in Fig. 7 where the three-axis relative displacement is plotted alongside the two-axis inclination measurements.

3.3 Auxiliary weather instruments

At select locations a Vaisala WXT520 compact all-in-one weather instrument has been installed to obtain a more detailed weather data record. This comprises ambient air temperature, air pressure, relative humidity, wind (speed and direction) and precipitation as well as a two four-component net radiometer Kipp & Zonen CNR4. The net radiometer is installed without capabilities for ventilation and heating. The WXT520 is capable of heating the rain and wind sensor but for practical reasons this feature is only enabled when enough power is available which typically corresponds to good weather periods and turned off especially in prolonged bad-weather periods. Both instruments have been vendor calibrated and the respective calibration data are applied in the data conversion procedures as advised by the manufacturer.

https://doi.org/10.5194/essd-2021-176
Preprint. Discussion started: 11 June 2021

Open Access Earth System Science Data Discussions

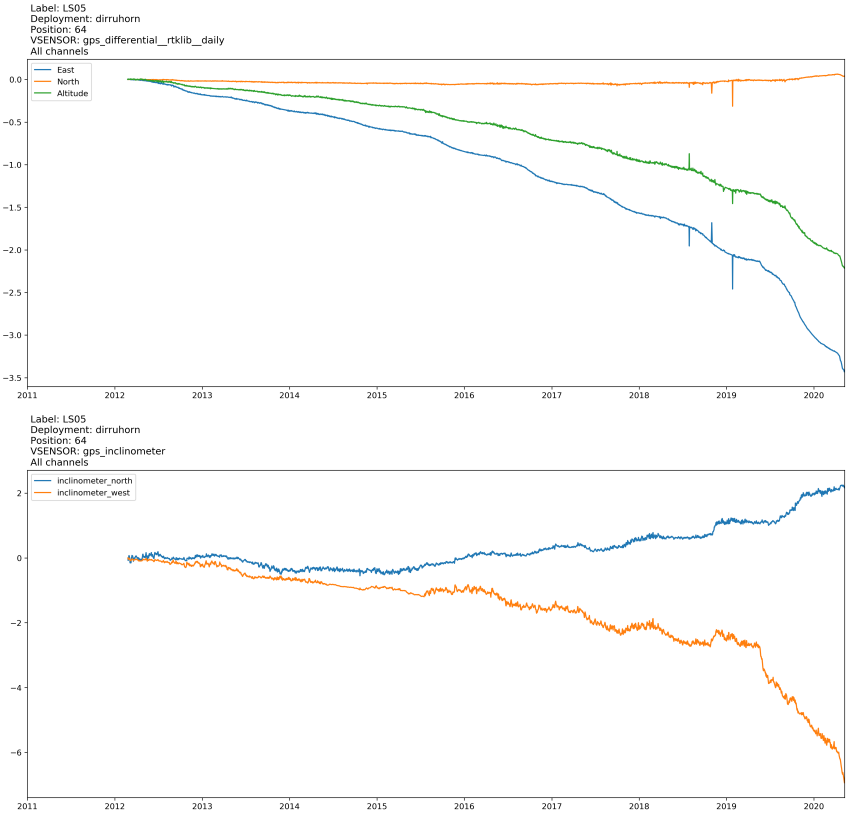

Figure 7. Daily coordinate series in east, north, altitude (top) as well as two-axis daily inclination values (bottom) for an accelerating landslide at Längschnee, Herbriggen (Switzerland) at 2611 m a.s.l. capture the kinematics in five degrees of freedom.

3.4 Local geodetic network

The most accurate position data can be computed using differential GNSS processing techniques when correction data from GNSS receiver with known position is available in close proximity to the one being computed (short baseline) (Wirz et al., 2013; Bu et al., 2021). For the chosen approach using single frequency GNSS receivers a short baseline on the order of hundreds of meters to max. a few kilometers is crucial as contrary to dual frequency receivers it is the sole possibility to mitigate atmospheric errors in the solutions to be obtained. Furthermore the preferably non-moving position reference and rover receiver should be situated in the same altitude regime, exhibit similar shading by topographic obstacles (sky view) and need to be operated in overlapping time windows for the best results.

Due to the aforementioned factors a set of local position references has been selected and equipped with continuously operating GNSS receivers as well as high-bandwidth data transmission (see Table 1 and Fig. 9). Together with select stations from the Permanent GNSS network in Switzerland (AGNES) these reference positions form the local geodetic network that all GNSS positions are referenced against. Periodic checks against the national GNSS network have shown that all but two position

https://doi.org/10.5194/essd-2021-176
Preprint. Discussion started: 11 June 2021

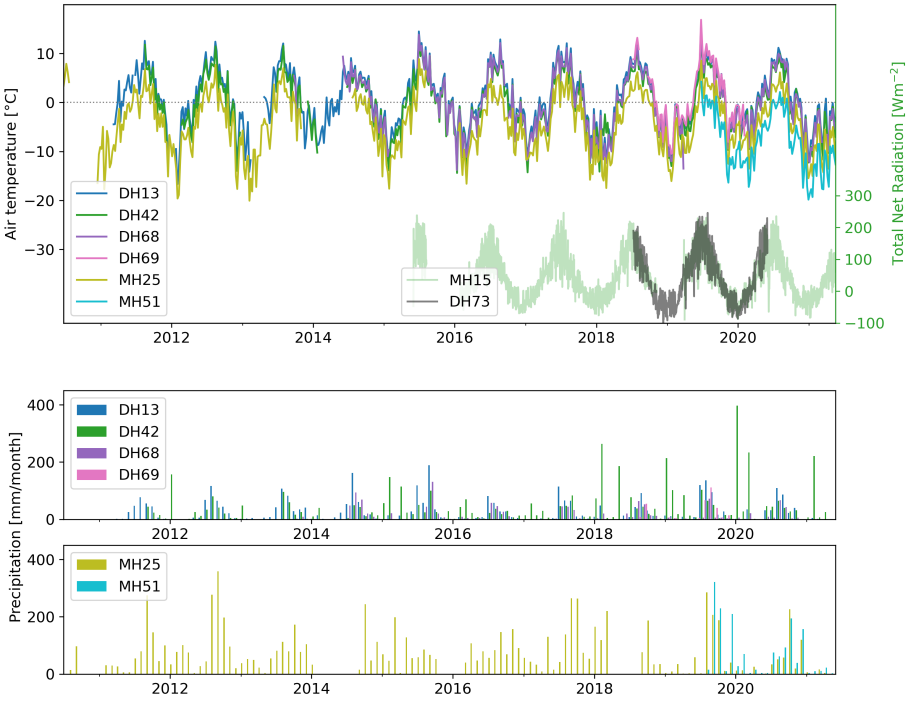

Figure 8. Ambient weather data from elevations between 2500 and 3500 m a.s.l (top). Precipitation at high altitudes is highly site specific and typically cannot be measured reliably in winter. Here we see data from different locations around the the rock glacier cluster in the Matter Valley (middle) as well as from Matterhorn (bottom).

Table 1. Local geodetic network: reference stations.

Reference	Area	Topographic Feature	Sensor	Period
RD01	next to Dirruhorn rock glacier	large bedrock feature	u-blox LEA-6T, Trimble Bullet III	03/2011 - ongoing
RL01	between Längschnee and Breithorn	fractured ridge	u-blox LEA-6T, Trimble Bullet III	08/2011 - 05/2013
RG01	above Grabengufer rock glacier	bedrock on ridge	u-blox LEA-6T, Trimble Bullet III	09/2011 - ongoing
RAND	top of Grossgufer	bedrock above rockfall	Leica GRX1200+, AR25 antenna	05/2011 - ongoing
HOGR	Hörnligrat ridge	rock buttress on ridge	Leica GRX1200+, AR10 antenna	12/2010 - ongoing

https://doi.org/10.5194/essd-2021-176
Preprint. Discussion started: 11 June 2021

reference locations are stable and non-moving. The station RL01 was abandoned after the initial discovery that contrary to the survey, the ridge it is located on is actually moving at a rate of a few centimeters per year. Station HOGR is special as it is located on a moving buttress on the Matterhorn Hörnligrat ridge and therefore position data calculated against this moving reference needs to be corrected against this moving reference position before further analysis (see (Weber et al., 2019a)).

Figure 9. Local reference station located next to the Dirruhorn rock glacier at 2706 m a.s.l., Herbriggen (Switzerland). The GPS reference receiver (including a backup) is mounted atop a large bedrock outcrop. Solar power, communication equipment, a webcam and weather station are co-located at this site. © PermaSense Project

3.5 Near-realtime data communication

Cellular network coverage is limited in remote high-mountain areas. Therefore a unique solution comprising of a wireless LAN (WLAN) backbone and a fine distribution using a low-power Wireless Sensor Network (WSN) was sought. Using this approach it is possible to reach back into areas in the back of side valleys that are interesting from the monitoring perspective but not covered w.r.t. connectivity. In select locations a backup using standard 3G/4G modems was further implemented as a safeguard. All locations serviced by the WLAN backbone have standard Internet Protocol (IP) connectivity facilitating the use of standard sensing equipment. For ease of maintenance a local WLAN hotspot is also available at these sites.

Since Wireless LAN equipment is consuming a lot of energy, the actual sensors are integrated with a custom low-power Wireless Sensor Network (WSN) operating on ISM-band radio transceivers and a specialized communication protocol for data gathering (Beutel et al., 2009). Using a hierarchical system of commodity components for the backbone and a highly optimized and custom network for the fine distribution to spatially separated sensing locations it is possible to operate on a much reduced resource footprint and overlong periods of time without interventions. Details about the wireless data communication backbone are shown in Fig. 10.

https://doi.org/10.5194/essd-2021-176
Preprint. Discussion started: 11 June 2021

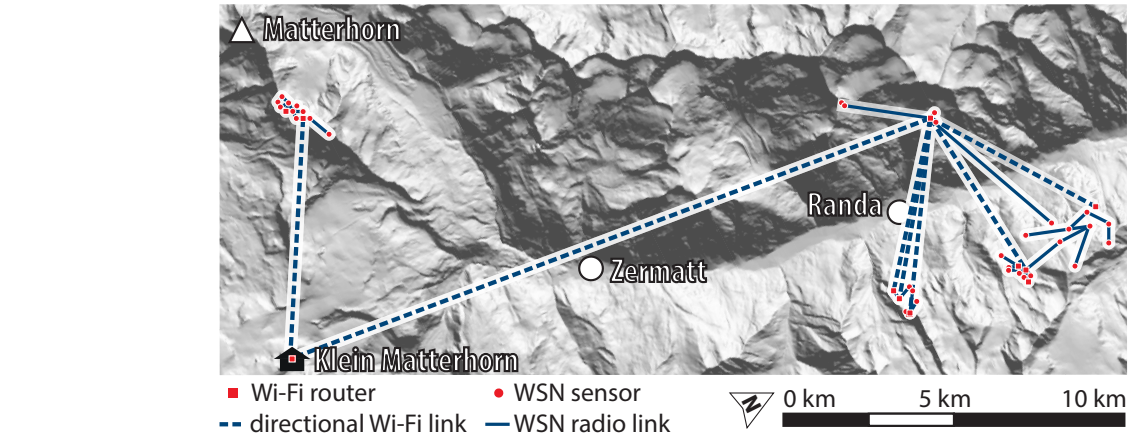

Figure 10. Wireless LAN backbone and fine distribution of wireless connectivity to all sensor locations in the Matter Valley.

3.6 Data management infrastructure

The data from all sensors is collected in a central database and available online on a public webpage at http://data.permasense.ch. See (Weber et al., 2019a) for details on the anatomy of this data management infrastructure and also on how to access this data online.

3.7 Field site selection and prerequisites for in-situ GNSS sensor installation

Mounting an in-situ GNSS sensor on an observation point poses some minimum requirements: Most importantly an observation point chosen must be representative for the landform and kinematic observations to be made and the longevity anticipated for the measurement to be undertaken. Since the method of installing permanent instrumentation to select ground points differs from the method of repeat surveys on larger arrays of points using mobile or temporary equipment (Lambiel and Delaloye, 2004) care needs to be taken to select "meaningful" positions in the landscape. The additional two-axis inclination measurements included in the instruments of this study and the data published here is of great value in understanding the three-dimensional nature of the movement (rotation, translation) and devising an analysis methodology, e.g. (Wirz et al., 2014a).

Depending on the nature of this chosen position ranging from e.g. massive bedrock, a deep seated rock entrained by sediments, a glacier surface or a superficial boulder simply lying on the surface of the landscape care must be taken in analysing the data and especially the extrapolation on a landscape scale. In many cases this is not possible in a straightforward way and therefore the further use of this data must be undertaken carefully.

For mounting of the sensor a distinctive rock feature large and stable enough to install and preserve the instrument, e.g. a large, deep-rooted rock is preferred. For practical reasons anchoring a ground observation point in loose material, e.g. by driving stakes or pouring foundations has been ruled out. As can be easily seen in Fig. 11 a large enough and deeply rooted rock feature is not always readily available and therefore compromises have to be made. Depending on the anticipated snow

https://doi.org/10.5194/essd-2021-176
Preprint. Discussion started: 11 June 2021

Figure 11. In very active movement zones finding a single block to fix the measurement instrument can be challenging both w.r.t. longevity and w.r.t. the representativeness of the block selected for the movement of the larger landform in question. The two locations shown are very active zones in steep, frontal parts of two rock glaciers above Herbriggen (Switzerland): Dirruhorn rock glacier (left) and Breithorn/Bielzug rock glacier (right). © PermaSense Project

cover a longer or shorter masts using guy-lines for increasing the stability can be used as well. In extreme cases of blocks sliding on the surface or toppling along the surface it may be required to re-level a GNSS instrument back to vertical after some time (see Fig.11 right). Also, it may happen that a sensor location is actually destroyed, e.g. by rockfall (see Fig.11 left) or avalanches. Since both the detailed site selection as well as the persistence of a measurement location requires some experience and learning it must me mentioned that there are no easy, clear and concise guidelines that can be given here. From a technical perspective good visibility to the horizon in direction of the equator (southern sky when working on the northern hemisphere is required both for good and persistent satellite visibility as well as solar radiation for power generation.

4 Primary data products

This section gives an overview as well as details of the main sensor setup installed at the different field sites and describes the primary data provided within this paper. Table 2 provides an overview listing of the main sensor types used including their approximate period of operation, units derived, measurement interval and key sensor characteristics. Tables 3, 4 and give a detailed listing of the location-specific instrumentation detailing the number of sensing channels and sensor types available at

https://doi.org/10.5194/essd-2021-176
Preprint. Discussion started: 11 June 2021


Open Access Earth System Science Data Discussions

each position. For every sensor type used, a detailed discussion of the specifics of each sensor type as well as installation and location-specific information is given in section 6. Finally, Fig. 12, 13 give a graphical overview of the data availability for all primary data products contained in this paper.

Table 2. Overview list of the sensors used ordered by sensor type.

Sensor Type	Sensor	Period	Unit	Interval	Accuracy
L1/L2-GNSS observables; position coordinates	Leica GRX1200+ GNSS receiver, AR10/25 antenna	03/2011 - ongoing	m	30 s	n.a.
L1-GPS observables; position coordinates	u-blox LEA-6T, Trimble Bullet III antenna	12/2010 - ongoing	m	5 s, 30 s	n.a.
Inclination	Murata SCA830-D07 Inclinometer	03/2011 - ongoing	°	120 s	±30 mg
Air temperature	Vaisala WXT520	12/2010 - ongoing	°C	120 s	±0.3 °C
Barometric pressure	Vaisala WXT520	12/2010 - ongoing	hPa	120 s	±1 hPa
Relative humidity	Vaisala WXT520	12/2010 - ongoing	%RH	120 s	$\pm 3-5\%$ RH
Wind speed	Vaisala WXT520	12/2010 - ongoing	km/h	120 s	±3 % at 10 m/s
Wind direction	Vaisala WXT520	12/2010 - ongoing	°	120 s	±3° at 10 m/s
Precipitation	Vaisala WXT520	12/2010 - ongoing	mm	120 s	resolution 0.01 mm
Radiation	Kipp & Zonen CNR4	06/2015 - ongoing	W/m^2	120 s	non-linearity <1 %

4.1 GNSS raw observation data

The key primary data product of this paper are raw GNSS observations in the form of daily RINEX 2.11 files available for each station. These contain C1 and L1 as well as C1, L1, D1, S1, P2, L2, D2, and S2 observables of the L1 and L1/L2 GNSS receivers respectively. Position HOGR and RAND contains both GPS and GLONASS observation data for both L1 and L2 sampled at an interval of 30 s, while the remaining positions are tracked at intervals of 30 s for L1-GPS rover stations and to a large extent 5 s for L1-GPS reference stations[2]. Especially for the latter, this results in a very large amount of data but gives flexibility for detailed analysis and algorithm development especially in the space of real-time kinematics. Since the rover GNSS instruments employed (Wirz et al., 2013; Buchli et al., 2012) are not always sampling data, but rather configurable according to a schedule the number of samples generated per day varies according to the schedule used. The schedule is defined using hourly granularity with a minimum of one on-hour per day. Data are provided in daily per-station RINEX files.

4.2 Inclinometer data

The integrated two-axis inclinometers are sampled at 2 min intervals during periods at which the GNSS sensor is running. The schedule for the inclinometer data acquisition is the same as for the GNSS sensor. Data are provided in CSV files.

[2]Some L1-GPS reference stations have operated on configured sampling periods of 30 s as well as 5 s.

https://doi.org/10.5194/essd-2021-176
Preprint. Discussion started: 11 June 2021

Open Access Earth System Science Data Discussions

4.3 Weather station data

The weather station data is originating from Vaisala WXT520 compact all-in-one weather instruments comprising ambient air temperature (see black line in Fig. 8), air pressure, relative humidity, wind (speed and direction) and precipitation as well as four-component net radiometers Kipp & Zonen CNR4. The raw weather station data sampled at 2 min intervals is provided in the form of CSV files.

4.4 Primary data product inventory

As described in Sec. 2 and also visible in Fig. 12 and 13, the sensor setup and number of field site has continuously grown over the years. There are a number of discontinued sensor locations and a few data gaps. The data yield and reliability of the measurement systems have surpassed expectations. For the sake of completeness it must be said that a few other sensor placements exist(ed), but due to their experimental nature and/or instability they are not part of this publication. The naming of all locations and data files follows the usual convention in GNSS data with four alphanumerical characters representing the station label prefixing the filenames, e.g. BH10 as prefix for `BH10_gps_inclinometer_2018.csv` containing GPS inclinometer data for the year 2018. A listing of stations and primary data products included in this paper is shown in Table 3 and 4, the structure of the data repository is explained in Sec.7.

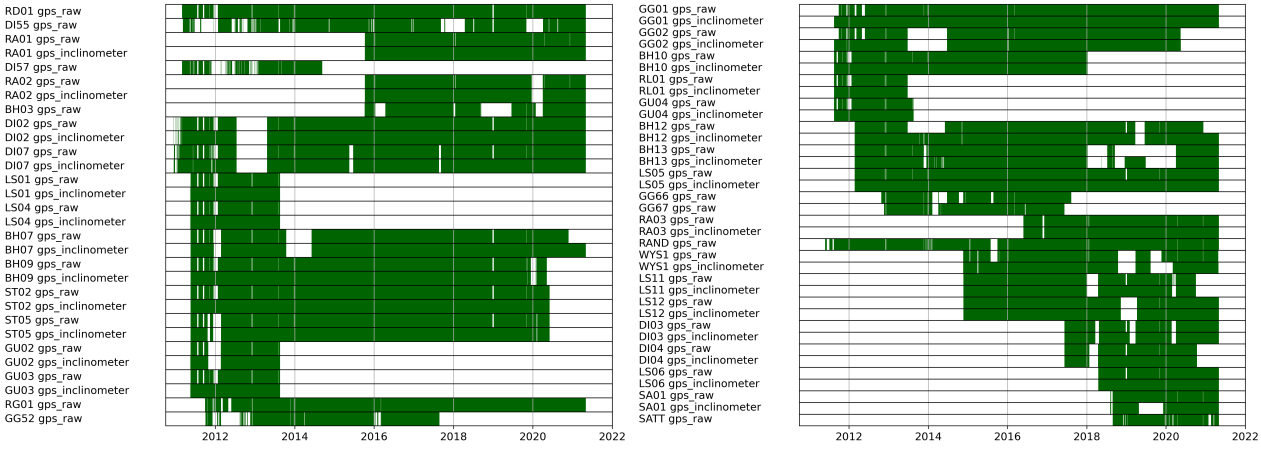

Figure 12. Data availability for all primary data products. The time periods when data are available are indicated in green (part 1).

5 Derived data products, data processing, cleaning and validation methodology

Raw sampled data typically needs to be processed to be usable for analysis purposes. This processing consists of data transformations as well as cleaning, aggregation and validation steps. In the case of this data set the main data transformation step performed on the raw primary GNSS data is to calculate daily static GNSS positions using double-differential GNSS post-

https://doi.org/10.5194/essd-2021-176
Preprint. Discussion started: 11 June 2021

Open Access Earth System Science Data Discussions

Table 3. Per position overview of sensor channels: Part 1.

Station	Period of operation	Reference	Online data	Location[a]			Kinematics			Weather	
				East	North	Altitude	L1/L2-GNSS	L1-GPS	Inclination	Radiation	Weather data
RD01	2011-03-01 - ongoing	RAND	X	2629577.9732	1108071.9804	2706.7478		X			
DI55	2011-03-09 - ongoing	RD01	X	2629457.1762	1107876.5744	2694.2237		X			
RA01	2015-10-08 - ongoing	RAND	X	2625797.1934	1107096.7129	2326.1968		X	X		
DI57	2011-03-01 - 2014-09-11	RD01		2629354.5315	1107816.5825	2673.0156		X			
RA02	2015-10-08 - ongoing	RAND	X	2625772.6134	1107086.6836	2336.0758		X	X		
BH03	2015-10-07 - ongoing	RD01	X	2629378.2574	1109934.4929	2754.6754		X	X		
DI02	2011-05-02 - ongoing	RD01	X	2629569.1061	1107710.4629	2770.3198		X	X		
DI07	2010-12-16 - ongoing	RD01	X	2629355.9386	1107810.8851	2673.3196		X	X		
LS01	2011-05-18 - 2013-08-19	RD01		2629465.3402	1109281.1964	2804.9886		X	X		
LS04	2011-05-18 - 2013-08-19	RD01		2629455.3763	1109179.2414	2802.0286		X	X		
BH07	2011-05-18 - ongoing	RD01	X	2629787.0910	1110178.9898	2982.6222		X	X		
BH09	2011-05-18 - ongoing	RD01	X	2630158.3320	1110218.1338	3159.6866		X	X		
ST02	2011-05-18 - ongoing	RD01		2630157.1405	1108556.4447	2997.0453		X	X		
ST05	2011-05-18 - ongoing	RD01		2630237.4437	1108650.9804	3029.1299		X	X		
GU02	2011-05-18 - 2013-05-24	RD01		2629715.8630	1109034.6960	2969.0446		X	X		
GU03	2011-05-18 - 2013-05-24	RD01		2629761.3476	1108988.3908	2996.2968		X	X		
RG01	2011-09-29 - ongoing	RAND	X	2628984.9027	1104371.2055	2974.2334		X			
GG52	2011-10-03 - 2016-12-30	RG01		2628872.3578	1104514.0648	2894.2230		X			
GG01	2011-09-29 - ongoing	RG01	X	2628937.0924	1104474.4768	2906.7283		X	X		
GG02	2011-09-29 - 2020-05-17[b]	RG01	X	2628872.2392	1104513.8539	2894.2559		X	X		
BH10	2011-08-17 - 2018-01-08[c]	RD01	X	2629255.8182	1109755.1909	2662.8449		X	X		
RL01	2011-08-17 - 2013-05-24	RD01		2629491.4431	1109569.5607	2873.8954		X	X		
GU04	2011-08-17 - 2013-05-24	RD01		2629946.0037	1108966.2652	3130.6487		X	X		
BH12	2012-02-24 - ongoing	RD01	X	2629596.1092	1110114.9246	2872.2844		X	X		
BH13	2012-02-24 - ongoing	RD01	X	2629332.5196	1109779.7778	2701.7375		X	X		
LS05	2012-02-24 - ongoing	RD01	X	2629059.8147	1109378.9914	2611.4904		X	X		
GG66	2012-10-26 - 2016-12-30	RG01	X	2628817.1390	1104430.3734	2905.9313		X			
GG67	2012-11-20 - 2016-12-30	RG01	X	2628782.6573	1104448.0691	2889.1460		X			
RA03	2016-05-27 - ongoing	RAND	X	2625736.1438	1107044.3597	2325.6056		X	X		
RAND	2011-05-28 - ongoing	ZERM[d]	X	2625632.6476	1107181.3446	2415.0521	X				
WYS1	2014-11-20 - ongoing	RAND	X	2624011.3148	1105068.5083	3056.8784		X	X		
LS11	2014-11-21 - 2020-10-03[b]	RD01	X	2629018.7584	1109451.0003	2588.5077		X	X		
LS12	2014-11-21 - ongoing	RD01	X	2629053.8167	1109268.3039	2604.1409		X	X		

[a] Location coordinates are given for the first day of deployment. [b] Sensor location detached in a rockfall ending the time series. [s] Sensor was destroyed in an avalanche ending the time series. [d] Data from the Permanent GNSS network in Switzerland (AGNES) is used here.

https://doi.org/10.5194/essd-2021-176
Preprint. Discussion started: 11 June 2021

Open Access Earth System Science Data Discussions

Table 4. Per position overview of sensor channels: Part 2.

Station	Period of operation	Reference	Online data	Location[b]			Kinematics			Weather	
				East	North	Altitude	L1/L2-GNSS	L1-GPS	Inclination	Radiation	Weather data
DI03	2017-06-09 - ongoing	RD01	X	2629354.9674	1107798.8201	2676.1565		X	X		
DI04	2017-06-09 - ongoing	RD01	X	2629241.3838	1107861.5433	2599.9488		X	X		
LS06	2018-04-17 - ongoing	RD01	X	2628942.5273	1109255.5280	2524.1405		X	X		
SA01	2018-08-06 - ongoing	RAND	X	2628397.6095	1099584.4213	3079.6403		X	X		
SATT	2018-08-29 - ongoing	RAND	X	2628357.9625	1099535.3189	3127.5589		X	X		
DH13	2011-03-08 - ongoing		X	2629563	1108035	2690					X
DH42	2011-08-17 - ongoing		X	2628985	1104370	2827					X
DH68	2013-08-20 - ongoing		X	2629598	1110119	2870					X
DH69	2018-07-10 - 2020-06-03		X	2629385	1107919	2644					X
DH73	2018-07-10 - 2020-06-03		X	2629385	1107919	2644				X	
DIS1	2012-07-19 - ongoing	RD01		2632748.4992	1115588.9891	2426.9658		X	X		
DIS2	2012-07-19 - ongoing	RD01		2632911.5828	1115403.7156	2501.0427		X	X		
RIT1	2012-07-19 - ongoing	RD01		2631650.5644	1113771.6430	2605.7951		X	X		
GRU1	2012-07-25 - ongoing	RD01		2640436.7470	1113468.7938	2823.0919		X	X		
JAE1	2012-07-26 - ongoing	RD01		2639856.8628	1111235.7781	2585.0723		X	X		
SCH1	2012-08-04 - ongoing	SAME[a]		2791062.5911	1152725.5875	2809.2476		X	X		
MUA1	2012-08-04 - ongoing	SAME[a]		2791144.4176	1153620.4315	2609.6384		X	X		
LAR1	2014-09-26 - ongoing	SANB[a]		2718881.9604	1148509.0717	2355.8913		X	X		
LAR2	2014-09-28 - ongoing	SANB[a]		2718731.2462	1148483.4638	2304.4097		X	X		
COR1	2015-12-17 - ongoing	SAME[a]		2783147.4647	1144727.7691	2669.5887		X	X		
MH15	2015-06-02 - ongoing		X	2618019	1092200	3402				X	
MH25	2010-12-17 - ongoing		X	2618019	1092200	3402					X
MH51	2019-06-26 - ongoing		X	2617392	1091918	4003				X	
MH33	2014-08-16 - ongoing	HOGR	X	2617961.1076	1092175.3683	3487.9016		X	X		
MH34	2014-08-14 - ongoing	HOGR	X	2618001.6299	1092197.6519	3463.7656		X	X		
MH35	2015-06-02 - ongoing	HOGR	X	2617961.1076	1092175.3683	3487.9016		X	X		
MH40	2015-06-03 - ongoing	HOGR	X	2617957.2225	1092175.2147	3489.2911		X			
HOGR	2011-02-03 - ongoing	ZERM[a]	X	2618012.5286	1092200.7753	3463.1838	X				
MH43	2018-08-15 - 2020-07-08	HOGR	X	2617957.1890	1092175.2476	3489.5281		X			

[a] Data from the Permanent GNSS network in Switzerland (AGNES) is used here. [b] Location coordinates are given for the first day of deployment for GNSS stations and manually measured instrument locations for other sensors.

https://doi.org/10.5194/essd-2021-176
Preprint. Discussion started: 11 June 2021

Open Access Earth System Science Data Discussions

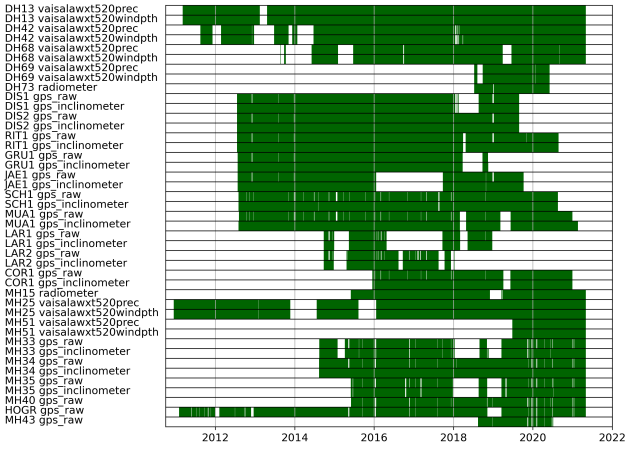

Figure 13. Data availability for all primary data products. The time periods when data are available are indicated in green (part 2).

processing and to clean and downsample all remaining primary data to usable formats and time scales. These steps as well as the tooling used are explained in the following.

5.1 GNSS computed daily positions

Apart from the raw GNSS observations in the form of daily RINEX 2.11 files we provide a derived data product, namely calculated daily positions for all GNSS sensors. Daily static positions are calculated using double-differential GPS post processing. Double-differential GNSS processing (Teunissen and Montenbruck, 2017) is based on data obtained in a common observation interval from a station pair. Positions for the so-called "rover" station can be calculated with high accuracy under the assumption that the "reference" station location is quasi-stationary and that observations from both stations are subject to similar perturbations. In practical application of this technique care should be taken that the baseline distance between any station pair is short, the field of view to the satellites (horizon) is similar and that a station pair be located in the same altitude regime. The main quality indicators of the input data (GNSS observables) are the number of visible satellites, the signal-to-noise ratio and the observation duration. For the derived data products the ratio of fixed ambiguities as well as the standard deviations per coordinate axis are key quality indicators. Double-differencing achieves best accuracy when utilizing the precision final GNSS data products from the International GNSS Service (IGS) although other GNSS data products can be used as well, e.g. if near-realtime solutions are required for warning purposes. The processing flow using two different post-processing tool chains, namely the Bernese GNSS Software (Dach et al., 2015) and the open-source RTKLIB toolchain[3] are described in the following as well as shown in figure 14.

We provide the scripts and configuration files used to run the open-source RTKLIB toolchain both from the RINEX files contained in this dataset as well as from the online data from the PermaSense database (see Sec. 7 and Appendix B). The post processing bases on daily observation files with one file per day and position compiled from the online database. To constitute

[3]http://www.rtklib.com

https://doi.org/10.5194/essd-2021-176
Preprint. Discussion started: 11 June 2021

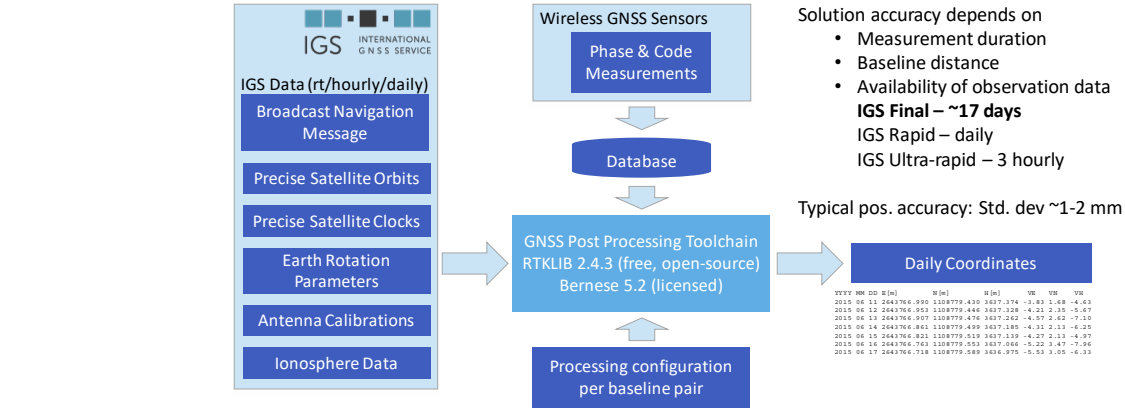

Figure 14. Typical GNSS post-processing workflow using the Bernese GNSS Software or RTKLIB.

a baseline pair between a rover position and a stable reference, typically a reference from the local geodetic network is used. In exceptional cases, e.g. to reference the local geodetic network references or when the baseline distance is high reference positions from the permanent GNSS network in Switzerland (AGNES) are used (see Tables 3 and 4). In a final step the position coordinates are converted from WGS84 coordinates to Swiss national coordinates using the online REFRAME conversion service (REST API) by swisstopo. The geodetic datum of all daily position data is CH1903+/LV95 with the reference frame Bessel (ellipsoidal). After post-processing data for each position are collated into a single CSV file that are available in the folder `gnss_data_raw` or are uploaded again to the PermaSense database for convenient online data access. The output format of the position data CSV files is described in Table 5, an example is shown here:

```
time,position,label,processing_time,device_type,version,reference_label,e,n,h,sd_e,sd_n,sd_h,ratio_of_fixed_ambiguities
2019-01-08T12:00:00Z,25,BH07,1578308717385,wireless-gps,4,RD01,2629785.13300,1110178.03760,2981.84610,0.00210,0.00300,0.00450,20.00000
2019-01-09T12:00:00Z,25,BH07,1578308867196,wireless-gps,4,RD01,2629785.13010,1110178.03810,2981.83850,0.00220,0.00310,0.00490,213.40000
2019-01-10T12:00:00Z,25,BH07,1578308942042,wireless-gps,4,RD01,2629785.12750,1110178.03860,2981.84350,0.00330,0.00410,0.00630,7.60000
2019-01-11T12:00:00Z,25,BH07,1578308946489,wireless-gps,4,RD01,2629785.12810,1110178.03800,2981.83850,0.00220,0.00270,0.00460,27.50000
```

The processing using the Bernese GNSS software is a similar process but due to the license-only availability and the complexity of the Bernese toolchain details are omitted here. Due to the two processing tools using different algorithms, code implementation and parameter sets, the output data is slightly different. This is most noticeable as due to different parameter threshold settings, it may happen that a daily computed position is available for a given day and tool, but not vice versa. Given the long-term nature of the observations these often spurious missing values can be safely interpolated in a further processing step if deemed necessary by the application.

5.2 PermaSense Data Manager - Managing and cleaning of the dataset

A generic toolchain to access, compile, clean, aggregate and validate both primary as well as derived data from the online PermaSense database has been developed (Weber et al., 2018a)[4]. This tool allows to query the database based on location

[4]https://gitlab.ethz.ch/tec/public/permasense/permasense_datamgr

https://doi.org/10.5194/essd-2021-176
Preprint. Discussion started: 11 June 2021

Value	Unit	Description
time		Timestamp of the position data
position		Inventory position number from the database
label		Station label
processing_time	milliseconds	Processing time in Unix time in milliseconds
device_type		Sensor type
version		Processing framework version
reference_label		Reference station label
e	m	Easting
n	m	Northing
h	m	Altitude
sd_e	m	Standard deviation Easting
sd_n	m	Standard deviation Northing
sd_h	m	Standard deviation Altitude
ratio_of_fixed_ambiguities		Quality metric from post-processing

Table 5. GNSS computed daily position data CSV file format.

and sensor type/data type, compile raw CSV files, apply metadata, data cleaning and correction functions, aggregate time-series data to pre-selectable aggregation intervals and produce intuitive validation plots. The data cleaning and correction step allows to delete outliers based on time intervals or value thresholds as well as perform simple mathematical corrections, e.g. to apply a constant factor or an offset for a given interval. Using this latter feature allows to correct artifacts introduced during site maintenance, e.g. from changing sensor equipment or from re-levelling a GNSS mast that is required when the tilt angle changes very much. An example for such a correction is shown in Fig. 15 for the north component of the inclinometer data of station BH10 that is located on the very instable tongue of the Gugla/Bielzug rock glacier (see Fig. 11 left). The corresponding correction metadata file is given below:

```
depo,vsensor,var,time_beg,time_end,cond_op,cond_par,op,par,comment,checked,,
dh55,gps_inclinometer,inclinometer_north,,2011-08-18,,,del,,,,,
dh55,gps_inclinometer,inclinometer_north,2011-08-18,2012-02-23,,,offset,0.7,,,,
dh55,gps_inclinometer,inclinometer_north,2012-02-23,2012-02-24,,,del,,device_change,,,
dh55,gps_inclinometer,inclinometer_north,2012-02-24,2012-07-17,,,offset,-0.55,,,,gitl
dh55,gps_inclinometer,inclinometer_north,2012-07-17,2012-07-19,,,del,,leveled_mast,,,
dh55,gps_inclinometer,inclinometer_north,2012-07-19,2013-06-26,,,offset,3.9,,,,
dh55,gps_inclinometer,inclinometer_north,2013-06-26,2013-06-27,,,del,,gps_logger_to_WGPS,,,
dh55,gps_inclinometer,inclinometer_north,2013-06-27,2014-06-05,,,offset,7.7,,,,
dh55,gps_inclinometer,inclinometer_north,2013-07-24,2013-07-25,,,del,,outlier,,,
dh55,gps_inclinometer,inclinometer_north,2014-06-05,2014-06-07,,,del,,leveled_mast,,,
dh55,gps_inclinometer,inclinometer_north,2014-06-07,,,,offset,-12,,,,
```

https://doi.org/10.5194/essd-2021-176
Preprint. Discussion started: 11 June 2021

Here, outliers from days with sensor device changes are removed using the `del` operation and offsets due to differences between two sensor devices are corrected using the `offset` operation. The original data is visible in orange while the cleaned data is visible in green and the aggregate over 1400 minutes (daily values) is shown in red in Fig. 15. The resulting aggregated time series is nice and smooth as well as continuous, largely without artifacts like jumps or excessive noise from bad weather periods where the stronger wind is perturbing the inclinometer readings (see small green spikes in Fig. 15). A quick tutorial for this tool is given in A.

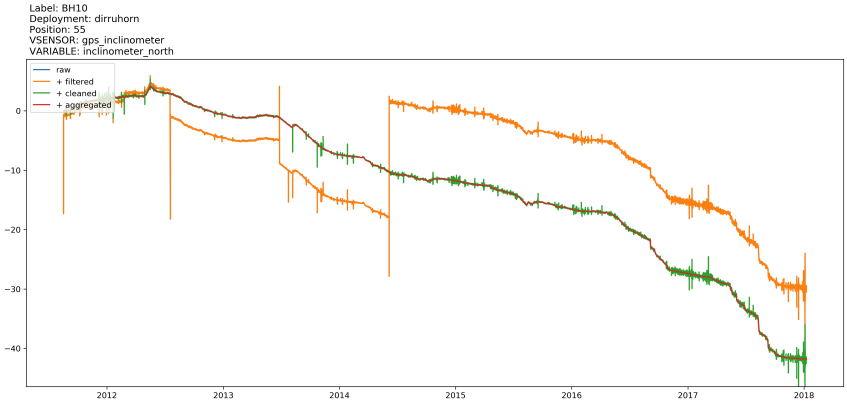

Figure 15. Data cleaning example: Inclinometer north component time series data for location BH10 on the Gugla/Bielzug rock glacier has severe outliers and jumps in the raw data that can be removed, compensated for and aggregated to smooth time series using the PermaSense Data Manager.

5.3 Cleaned and aggregated GNSS daily positions

All GNSS derived daily positions are converted to relative coordinates starting with a zero value at the start of the measurement period and have undergone a rudimentary data cleaning step: Outliers and jumps pertaining from device changes on field service days have been removed. An example of the output CSV file format is shown here:

```
time,position,label,processing_time,device_type,version,reference_label,e,n,h,sd_e,sd_n,sd_h,ratio_of_fixed_ambiguities
2019-01-08T12:00:00Z,25,BH07,1549509120000,wireless-gps,3,RD01,-1.9610,-0.9588,-0.7752,0.0002,0.0003,0.0005,95.5000
2019-01-09T12:00:00Z,25,BH07,1549595520000,wireless-gps,3,RD01,-1.9630,-0.9598,-0.7792,0.0002,0.0002,0.0004,100.0000
2019-01-10T12:00:00Z,25,BH07,1549681920000,wireless-gps,3,RD01,-1.9650,-0.9598,-0.7812,0.0001,0.0002,0.0004,100.0000
2019-01-11T12:00:00Z,25,BH07,1549768320000,wireless-gps,3,RD01,-1.9660,-0.9608,-0.7782,0.0001,0.0002,0.0004,100.0000
```

All cleaned daily position files are available in the folder `gnss_derived_data_products`.

5.4 Cleaned and aggregated inclinometer and weather station data

Similarly, the raw data from inclinometer and weather station sensors is available at 2 min sampling intervals. As described based on the example of the Gugla/Bielzug rock glacier earlier (see Sec.5.2 all time series data from inclinometer and weather

https://doi.org/10.5194/essd-2021-176
Preprint. Discussion started: 11 June 2021

Open Access Earth System Science Data Discussions

station are cleaned, offset-compensated and aggregated to hourly data products. All of these data files are available in the folder `timeseries_derived_data_products`.

5.5 Standardized analysis plots

For each position a number of standardized graphs are generated (see Fig. 7). These plots are available for all derived data products in the folder `timeseries_sanity_plots` of the data repository and also as supplement to this paper.

5.6 Inventory of derived data products

An inventory of all derived data products is available in Tables 3 and 4.

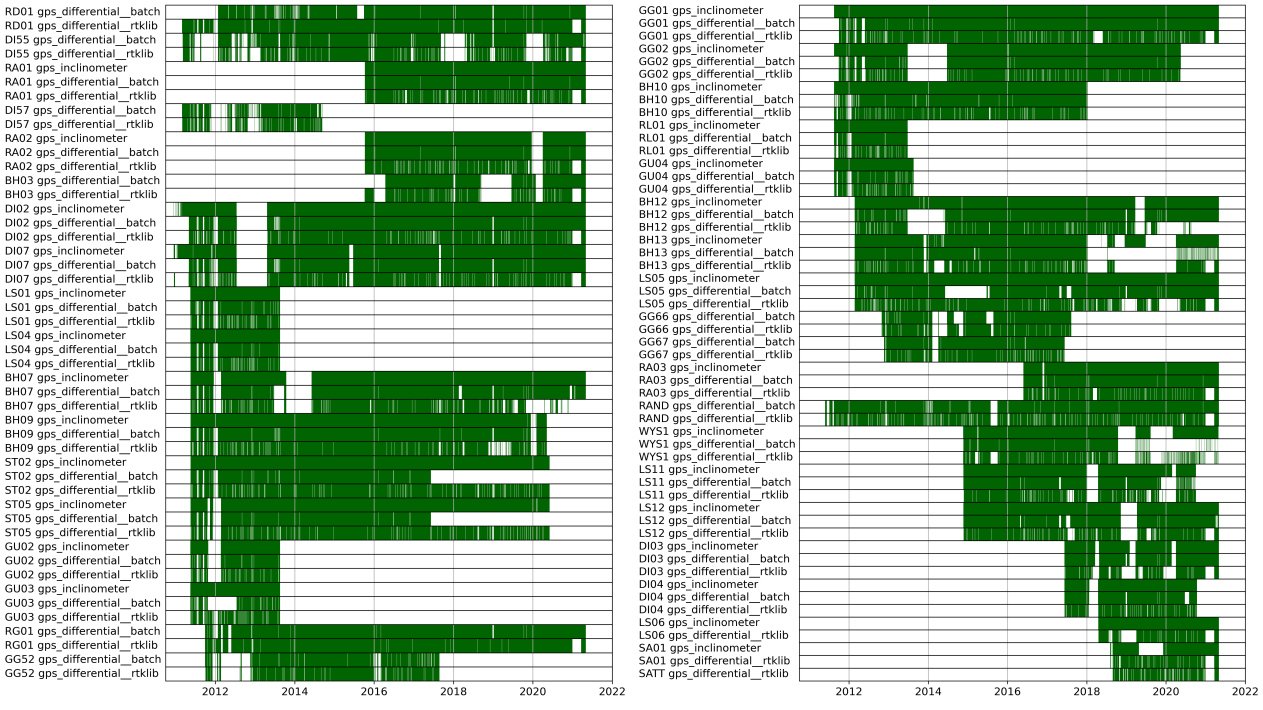

Figure 16. Data availability for all derived data products. The time periods when data are available are indicated in green.

6 Past work and scientific results based on this data set

The X-Sense project and its cross-pollination and technology transfer to further projects lead to a broad scientific output in the fields of electrical engineering, geomorphology, and geophysics as described earlier. In this section, we present a brief description of the scientific output as well as the scope of the projects organized by landform type. These references can be used as starting points to probe further and more detailed information.

https://doi.org/10.5194/essd-2021-176
Preprint. Discussion started: 11 June 2021

Open Access Earth System Science Data Discussions

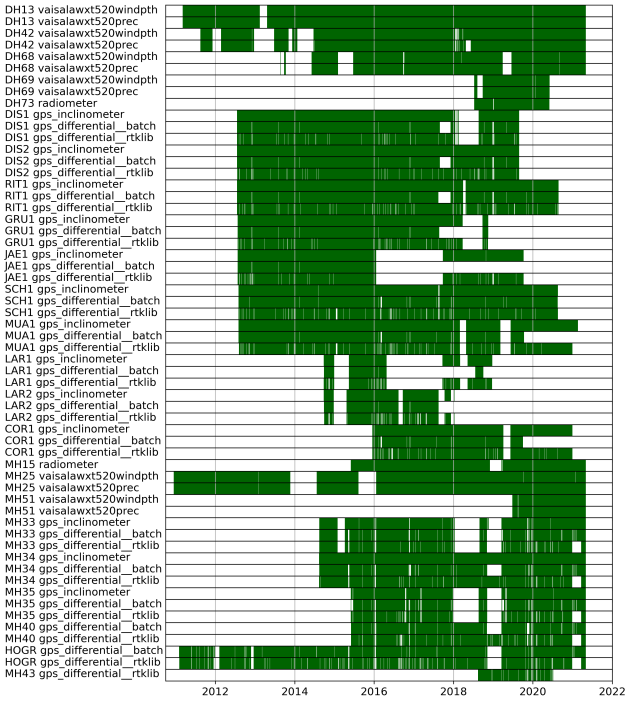

Figure 17. Data availability for all derived data products. The time periods when data are available are indicated in green.

6.1 Rock glaciers

Twelve rock glaciers across all of Switzerland have been instrumented with permanent GNSS sensors, many of which are still being actively monitored. The location of the rock glaciers varies from the Matter Valley in the western Swiss Alps, the central Gotthard region and also the eastern Swiss Alps. The Gugla/Bielzug, Dirruhorn, Grabengufer and Steintälli rock glaciers were initially equipped with a focus on process studies within the X-Sense project as described. Following this an extension to other rock glaciers was performed under the auspices of the Swiss Permafrost Monitoring Network (Noetzli et al., 2019). Many of the sites described below are also monitored using manual measurements. The respective data falls beyond the scope of this publication but can be obtained from the authors or from PERMOS.

A cluster of six rock glaciers (Gugla/Bielzug, Dirruhorn, Distelhorn, Ritigraben, Steintälli and Grabengufer rock glaciers) is concentrated in the right orographic side of Matter Valley. This valley is rich in rock glaciers, many of which move relatively rapidly, with average displacement rates up to several meters per year (Delaloye et al., 2013; Strozzi et al., 2020). These, as well as several other rock glaciers across the valley are directly connected to gullies, display large sediment transfer rates and ultimately expose the settlements and transportation system in the valley bottom to significant and periodic natural hazards. This cluster of rock glaciers form the basis of several publications regarding the monitoring technique developed (Wirz et al., 2013; Buchli et al., 2012) as well as first geomorphological studies and analysis methodology (Wirz et al., 2014b, a). Due to their high velocity and the exceptionally detailed data availability, they offer interesting possibilities to investigate the ongoing

https://doi.org/10.5194/essd-2021-176
Preprint. Discussion started: 11 June 2021

observed increases in the creep rates of mountain permafrost and several papers used these data for process understanding (Wirz et al., 2016).

The Dirruhorn rock glacier is a well studied landform, with peculiar kinematic behaviour (Delaloye et al., 2010). Continuous kinematic measurements are available since 2011 for three positions on the upper part and the first steep flank of the rock glacier. In the year 2018 two more positions were instrumented on the fast moving tongue, with the goal of creating a spatially resolved network for the analysis of the spatial variability of rock glacier velocities at a daily scale (Cicoira et al., 2019b, 2021).

The Steintälli rock glacier is located a few hundred meters higher in the same catchment as the Dirruhorn rock glacier. It is not directly connected to the valley bottom and is characterized by gentler slope gradients in comparison to the other rock glaciers in the valley. However it carries two exemplary steep frontal zones above which the two GNSS sensors are positioned. The creep rates and the seasonal variability of this rock glacier are less pronounced and are more related to the general patterns observed in the Alps rather than its steeper neighbours in the Matter Valley (Noetzli et al., 2019).

The Grabengufer is a complex landform comprising of a landslide (sagging) originating at approx. 2800 m a.s.l. as well as a very fast moving rock glacier releasing its debris into a hazardous debris flow ending just north of the village of Randa (Delaloye et al., 2013). It has seen mitigation measures for many decades with the earliest on record dating back to 1945 where a protective wall was constructed to fence off a lateral part of the moving rock glacier in the area of the "Grüne Garten" above the village of Randa [5]

The Gugla/Bielzug rock glacier is situated towards the north above the village of Herbriggen between the peaks of the Gugla and Breithorn. The frontal part of the rock glacier opens up into a very steep gully with frequent and high-volume discharge of loose material. The Gugla/Bielzug rock glacier and Bielzug debris flow are a serious hazard source in the area with. Significant efforts have been undertaken to (i) study the details and (ii) implement protective measures for the safety of the valley habitat and infrastructure. Specifically a debris catchment, several damming structures and an early warning system using geophones has been implemented (Kummert et al., 2018a; Kummert and Delaloye, 2018; Kummert et al., 2018b; Wirz et al., 2014b; Guillemot et al., 2021; Oggier et al., 2016).

The Ritigraben rock glacier is a well studied landform in the vicinity of the ski slopes of Grächen (Switzerland). In addition to the kinematics data, borehole temperatures and inclinometers data are available (Kenner et al., 2017, 2018; Cicoira et al., 2019a).

The Gruben and Jäggi rock glaciers are located in the adjacent Saas Valley, near Saas Grund, (Switzerland). They are among the first rock glaciers investigated in Switzerland (Haeberli et al., 1979; Haeberli, 1996, 1985; Haeberli and Schmid, 1988).

A second cluster of rock glacier is concentrated in upper Engadine (Murtel-Corvatsch, Muragl, Schafberg rock glaciers). The two valleys of Engadine and Matter Valley are the driest valley in Switzerland and being characterised by high mountain peaks, they host the majority of rock glaciers in the country (Haeberli and Vonder Mühll, 1996).

The Muragl rock glacier is located in the homonim valley in the municipality of Samedan (Switzerland). The rock glacier has been investigated already twenty years ago in some of the first detailed photogrammetric studies from aerial and satellite

[5] Protocol of the Swiss Federal Council, February 15, 1945.

https://doi.org/10.5194/essd-2021-176
Preprint. Discussion started: 11 June 2021

imagery in the periglacial environment (Kääb et al., 1997; Kaeaeb et al., 1998). On site, one fixed GNSS sensor is located a few hundred meters up from the PERMOS borehole (Cicoira et al., 2019a).

The Murtel-Corvatsch rock glacier is one of the first rock glaciers to be intensively studied worldwide. Its displacement rates are one to two orders of magnitude smaller than most other rock glaciers presented in this dataset. It hosts the longest time series of permafrost temperatures in an alpine rock glacier, dating back to 1987 (Vonder Mühll and Haeberli, 1990; Hoelzle et al., 2002). In the same years, also vertical inclinometer profiles were measured manually, providing a unique dataset. Recent detailed process oriented studies are based on the dataset presented (Cicoira et al., 2019a, 2021).

The Schafberg rock glacier is located above the municipality of Pontresina (Switzerland). The rock glacier delivers debris to steep slopes prone to snow avalanches and debris flows, that endanger the infrastructure and the village in the valley bottom. Therefore, it has been object of investigations from this and other projects related to natural hazards. The kinematics measurements are complemented by borehole temperatures and past inclinometer profile measurements (Arenson et al., 2002), available through PERMOS. Detailed studies about rock glacier dynamics have investigated this well monitored site (Cicoira et al., 2019a; Kenner et al., 2020).

The Largario rock glacier is located in the Adula/Rheinwaldhorn massif and therefore ads to the monitoring concept in a different weather zone (Scapozza et al., 2014). This rock glacier is known as an important source of debris reworked by debris flow descending the Soi Valley, and causing in the past several damages at the village of Dangio-Torre and destroing, the 28/29 August 1908, the chocolate plant located at the confluence of Soi Valley into the Blenio Valley.

6.2 Steep rock walls

Three field sites are focusing on steep bedrock walls. The situation, past research as well as the datasets of the Matterhorn Hörnligrat field site are described in detail in Weber et al. (2019a); Hasler et al. (2008, 2012); Talzi et al. (2007); Beutel et al. (2009); Weber et al. (2017). This dataset comprises the most comprehensive and longest duration dataset in mountain permafrost worldwide. The site is mainly clustered in and around a prominent high-alpine rockfall that took place in 2003. Apart from the thermal and kinematic measurements documented in Weber et al. (2019a) recent years have also seen experimentation with seismic sensors (Weber et al., 2018c, b).

The Randa Grossgufer is a $30 \times 10^6\ \mathrm{m}^3$ rockslide site on the orographic left side of the Matter Valley just opposite from the Dirruhorn rock glacier. It has been thoroughly investigated by numerous researchers (Willenberg et al., 2008b, a; Gischig et al., 2011b; Fäh et al., 2012-12; Gischig et al., 2011a; Moore et al., 2011; Burjánek et al., 2010; Eberhardt et al., 2004). Monitoring activity has increased in the past years with one GNSS reference and 3x GNSS sensor rovers situated at the lip of the detachment.

The Sattelspitz is a minor buttress on the west ridge above Täsch (Switzerland). Due to slope instabilities and hazard potential for the fresh water supply of the village of Täsch a kinematic monitoring has been set up at this site. A fix GNSS sensor has been installed on top of a rock tower that is currently showing the largest displacement rates on the rock face. The data have not been analysed in a scientific publication.

https://doi.org/10.5194/essd-2021-176
Preprint. Discussion started: 11 June 2021


Open Access Earth System Science Data Discussions

6.3 Landslides

A number of landslides landslides have been instrumented in the Matter valley with goal of monitoring instable and potentially dangerous slopes. The Breithorn landslide is situated north of the Gugla/Bielzug rock glacier. It is actively being monitored using GNSS.

One ridge line further south is the Gugla with a not very prominent summit of the same name. This area features a large, relict landslide that surged at least once in 1959 when the village of Herbriggen was evacuated for a number of days in mid-winter [6]. The lower parts of the slopes leading down from the Gugla are known as Längschnee, a sediment and debris rich area characterized by sharp steepening drop leading into the valley and towering above the village of Herbriggen. Here, the excessive downslope movement of the whole area poses a significant and real risk for the habitat in the valley. Important countermeasures apart from observation and monitoring have been recently undertaken, e.g. a protective dam is currently being constructed and a large boulder (Grosse Stei) in the area of Längschnee has been fixed by anchoring and concrete underfilling. This boulder is monitored since 2018 using a GNSS sensor as well.

The Wisse Schijen landslide is situated on the orographic left side of the Matter Valley at around 3100 m, to the West of Randa. A large landslide is affecting the top of the permafrost slope equipped with avalanche protection structures (8 rows of snow nets). These nets retain snow in the Wisse Schijen avalanche release area and protect numerous rows of steel snow bridges below. A GNSS sensor is situated in the centre of the landslide to monitor slope displacements in parallel to borehole inclinometer measurements.

7 Code and data availability

The data set published with this paper contains data from March 01, 2011 until May 20, 2021. An overview of the structure, file types and size of the data sets, for both the raw primary data and derived data products, is given in Table 6. Furthermore, the data set also contains the key metadata files for the field sites. Annual updates of this data set are planned (living data process). Using the toolset described in Sect. 5.2 and appendix A and using the online repository at http://data.permasense.ch (see (Weber et al., 2019a) for details), the data user can also create custom updates of the data set independently. Furthermore, a set of wrapper scripts for GNSS post-processing using the open-source RTKLIB toolchain[7] are described in Appendix B. This toolchain allows compute the double-differencing GNSS daily positions both from the RINEX files contained in this dataset as well as from the online data from the PermaSense database in a standalone fashion as well as on a compute cluster with SLURM.

The data sets as well as the toolset (code) for preparing, processing, validating and updating the data contained in this publication are available through the following providers and data links:

- Data set will be published through pangaea.de, the DOI process is pending. Therefore the temporary review dataset link is: https://fileshare.uibk.ac.at/d/70817c21eb01421cb6a5/

[6] Geologisches Gutachten, Dr. R.U. Winterhalter, Zurich, 1959, personal communication R. Allmendinger, Herbriggen, various news reports from 1959.
[7] http://www.rtklib.com

https://doi.org/10.5194/essd-2021-176
Preprint. Discussion started: 11 June 2021


Open Access Earth System Science Data Discussions

Table 6. Structure, description, formats and sizes of the data set components.

Directory	Data Description	Format	# Data Points	# Files	Size
gnss_data_raw	GNSS raw observations	RINEX 2.11	-	114'056	298.4 GB
gnss_derived_data_products	daily position data	csv	209'948[8]	763	23 MB
timeseries_data_raw	raw primary sensor data	csv	54'461'571	467	8.9 GB
timeseries_derived_data_products	sensor data after cleaning/aggregation	csv	3'067'585	411	148.5 MB
timeseries_sanity_plots	standard plots for all data	png	-	692	172.8 MB
dirruhorn_nodepositions.xlsx	general metadata file	xlsx	-	1	40 kB
matterhorn_nodepositions.xlsx	general metadata file	xlsx	-	1	40 kB
permos_nodepositions.xlsx	general metadata file	xlsx	-	1	40 kB
README.md	-	md	-	1	4 kB
Total	-	-	57'739'104	116'393	307.6 GB

The code for processing the data in this publication is available in:

- https://gitlab.ethz.ch/tec/public/permasense/permasense_datamgr
- https://gitlab.ethz.ch/tec/public/permasense/rtklib_processing

8 Conclusions

This paper documents a multi field-site, decade+ monitoring effort using in-situ GNSS sensors on different landforms in the Swiss Alps. A such this dataset constitutes the largest and highest fidelity dataset documenting mass movement by means of permanent ground measurement points, a method that has been developed and put into practice by the authors. The data is obtained mainly at mass movement sites in the cryosphere with a few placements at lower altitudes at or beyond the fringe of permafrost. Most of these sites are subject to further investigations using a multitude of methods, e.g. terrestrial surveys, seismic, time-lapse photography, UAV surveys, InSAR etc.. A basic overview of these field sites, methods employed, data available and the respective literature are documented in section 6 allowing to probe further. As such this dataset provides a significant step for future work and development of novel methods, further process understanding and help mitigate natural hazards as well as adaptation strategies due to climate change. The method and data presented here are currently in discussion through stakeholders at the International Permafrost Association (IPA) and the Global Terrestrial Network on Permafrost (GTN-P) to establish kinematic observations of the cryosphere as a further Essential Climate Variable (ECV) within the worldwide climate-monitoring program (GCOS/GTOS).

https://doi.org/10.5194/essd-2021-176
Preprint. Discussion started: 11 June 2021

Appendix A: PermaSense Data Manager

Code for the management and processing of data associated with this paper is available at https://gitlab.ethz.ch/tec/public/permasense/permasense_datamgr (Weber et al., 2019b). It contains both a Python toolbox for downloading and processing primary as well as secondary. The toolbox contains routines for the compilation, cleaning, aggregation and validation of both primary as well as derived data products from the online PermaSense database at http://data.permasense.ch into a local file system. Specifically the PermaSense data manager allows to:

- Query data from PermaSense GSN server and save them locally as CSV files
- Load the locally stored CSV files
- Filter according to reference values if available
- Clean data manually if needed
- Generate aggregates using an arithmetic mean (exceptions for weather data)
- Generate per-year CSV files for each position and datatype
- Generate standard plots for all positions as an intuitive sanity check
- Query images from the PermaSense database server, convert to JPEG and save them locally.

Some Python additional modules are required. Using anaconda you can install the requirements by executing the following command:

```
conda env create -f condaEnvironment.yaml
conda activate permasense_datamgr
```

Individual positions can be enabled/disabled in the main python file `manage_GSNdata.py`, the metadata for filtering and cleaning is contained in the folder `./metadata`. Finally the tool is run by:

```
python manage_GSNdata.py
```

By default data are generated in the directory `./data`.

Appendix B: GNSS Processing using the Open-source RTKLIB

A set of scripts automates the computation of double-differential static GNSS solutions using the open-source toolchain RTKLIB[9]. The scripts are configurable and can be run on a compute cluster using SLURM[10] to speed things up. Configuration files and especially paths are set up for specific processing of the PermaSense GNSS data contained in this dataset but can be adapted to other processing needs accordingly. Furthermore some double-differential baselines require specific observation data that is only available from SwissTopo and therefore not contained in this dataset.

[9] http://www.rtklib.com
[10] https://slurm.schedmd.com/

https://doi.org/10.5194/essd-2021-176
Preprint. Discussion started: 11 June 2021


Open Access Earth System Science Data Discussions

B1 Prerequisites

In order to run these scripts the following prerequisites must be installed:

- RTKLIB processing scripts https://gitlab.ethz.ch/tec/public/permasense/rtklib_processing
- RTKLIB can be obtained from http://www.rtklib.com/ or alternatively https://github.com/rtklibexplorer/RTKLIB
- RINEX file compression tools https://terras.gsi.go.jp/ja/crx2rnx.html

B2 Processing job configuration files

A single processing job always computes a daily position for a given baseline pair. There are two kinds of configuration files that are required for each processing job. A parameter file that specifies a baseline pair, data down-/upload location, starting dates, default directories and tools to use for processing as well as a RTKLIB configuration file that passes the right options and parameters to the post-processing tool `rnx2rtkp`.

B3 Processing wrapper script

The main processing wrapper script is responsible for downloading all required data, creating a local temporary compute space, executing the post-processing tool `rnx2rtkp`, upload of the resulting data to the PermaSense database and archiving input and output data as well as cleaning up the temporary file space.

```
compute_solution.sh -p [parameter_file] -d -b -r -c -f -u YYYY MM DD
#     -d: igs data download
#     -b: no data download and no conversion for the basestation
#     -r: no data download and no conversion for the roverstation
#     -c: no conversion
#     -f: use IGS final data product
#     -u: upload to GSN database
```

B4 Automation on a compute cluster using SLURM

In order to automate the processing of multiple baseline pairs and multiple days at once the processing wrapper script can be embedded into further wrapper scripts that allows processing on a compute cluster using SLURM. The following script can be called with the SLURM command `sbatch` to compute multiple baseline pairs in one joint command for a given day using either the IGS final or rapid data products as well as with options for downloading and uploading. A further integration, e.g. for [processing multiple days at once is straightforward. An example is provided.]

```
slurm_gps_compute.sh -f -u -d YYYY DoY
#     -f: use IGS final data product
#     -u: upload to GSN database
#     -d: igs data download
```

https://doi.org/10.5194/essd-2021-176
Preprint. Discussion started: 11 June 2021

Open Access Earth System Science Data Discussions

```
#Configuration file with parameters used in order to download and convert data
[positions]
rover_station_deployment: cogear
rover_gsn_server:
rover_station_nr:         42
rover_station_label:      HOGR
rover_start_date:         02.02.2011
rover_gsn_upload_server:  data.permasense.ch
rover_gsn_upload_port:    22503

base_station_deployment:  pnac
base_gsn_server:
base_station_nr:
base_station_label:       ZERM
ref_pos_x:                4399182.5043
ref_pos_y:                597294.9166
ref_pos_z:                4566748.4823

[servers]
#clk, sp3 and erp files
dataserver_1=ftp://gssc.esa.int/igs/products
#nav files
dataserver_2=ftp://gssc.esa.int/igs/data/daily
#dcb files
dataserver_3=ftp://ftp.aiub.unibe.ch/CODE
#iono files
dataserver_4=ftp://gssc.esa.int/gnss/products/ionex

[directories]
igs_data_dir:           /ifi-NAS/nes/research/gps/external_dataproducts/igs_data
igr_data_dir:           /ifi-NAS/nes/research/gps/external_dataproducts/igr_data
code_data_dir:          /ifi-NAS/nes/research/gps/external_dataproducts/code_data
rtklib_dir:             /ifi-NAS/nes/research/gps/rtklib_processing/bin
rtklib_options_dir:     /ifi-NAS/nes/research/gps/rtklib_processing/bin/config
gps_data_dir:           /ifi-NAS/nes/research/gps/rtklib_processing
output_dir:             /ifi-NAS/nes/research/gps/rtklib_processing

[files]
rtklib_conf_file:       rtkpost_static_ZERM.conf
```

Figure B1. The parameter file specifies the processing baseline pair.

https://doi.org/10.5194/essd-2021-176
Preprint. Discussion started: 11 June 2021

Open Access Earth System Science Data Discussions

```
# rtkpost options (v.2.4.3)
pos1-posmode       =static     # (0:single,1:dgps,2:kinematic,3:static,4:static-start,5:movingbase,6:fixed,7:ppp-kine,8:ppp-static,
pos1-frequency     =3         # (1:l1,2:l1+l2,3:l1+l2+l5,4:l1+l5)
pos1-soltype       =combined   # (0:forward,1:backward,2:combined)
pos1-elmask        =15         # (deg)
pos1-snrmask_r     =on         # (0:off,1:on)
pos1-snrmask_b     =on         # (0:off,1:on)
pos1-snrmask_L1    =40,40,40,40,40,40,40,40,40
pos1-snrmask_L2    =40,40,40,40,40,40,40,40,40
pos1-snrmask_L5    =40,40,40,40,40,40,40,40,40
pos1-dynamics      =off        # (0:off,1:on)
pos1-tidecorr      =on         # (0:off,1:on,2:otl)
pos1-ionoopt       =brdc       # (0:off,1:brdc,2:sbas,3:dual-freq,4:est-stec,5:ionex-tec,6:qzs-brdc,7:qzs-lex,8:stec)
pos1-tropopt       =est-ztd     # (0:off,1:saas,2:sbas,3:est-ztd,4:est-ztdgrad,5:ztd)
pos1-sateph        =precise    # (0:brdc,1:precise,2:brdc+sbas,3:brdc+ssrapc,4:brdc+ssrcom)
pos1-posopt1       =on         # (0:off,1:on)
pos1-posopt2       =on         # (0:off,1:on)
pos1-posopt3       =precise    # (0:off,1:on,2:precise)
pos1-posopt4       =on         # (0:off,1:on)
pos1-posopt5       =on         # (0:off,1:on)
pos1-posopt6       =on         # (0:off,1:on)
pos1-navsys        =7          # (1:gps+2:sbas+4:glo+8:gal+16:qzs+32:comp)
pos2-armode        =3 #fix-and-hold # (0:off,1:continuous,2:instantaneous,3:fix-and-hold)
pos2-gloarmode     =on         # (0:off,1:on,2:autocal,3:fix-and-hold)
pos2-arfilter      =on         # (0:off,1:on)
pos2-arthres       =3
pos2-arthres1      =0.9999
pos2-arthres2      =0.25
pos2-arthres3      =0.1
pos2-arthres4      =0.05
pos2-varholdamb    =0.01       # (cyc^2)
pos2-gainholdamb   =0.01
pos2-arlockcnt     =5          # 0 for ublox, 5 else
pos2-minfixsats    =6
pos2-minholdsats   =7
pos2-mindropsats   =8
pos2-rcvstds       =on         # (0:off,1:on)
pos2-arelmask      =20         # (deg)
pos2-arminfix      =25
pos2-armaxiter     =2
pos2-elmaskhold    =20         # (deg)
pos2-aroutcnt      =100
pos2-maxage        =309        # (s)
pos2-syncsol       =off        # (0:off,1:on)
pos2-slipthres     =0.05       # (m) was 0.05 0.01
pos2-rejionno      =0.1        # (m)
pos2-rejgdop       =5
pos2-niter         =2          # was 2
out-solformat      =llh        # (0:llh,1:xyz,2:enu,3:nmea)
```

Figure B2. The rtkpost options file specifies the processing options - part 1.

https://doi.org/10.5194/essd-2021-176
Preprint. Discussion started: 11 June 2021


```
out-outhead       =on         # (0:off,1:on)
out-outopt        =on         # (0:off,1:on)
out-outvel        =off        # (0:off,1:on)
out-timesys       =gpst       # (0:gpst,1:utc,2:jst)
out-timeform      =hms        # (0:tow,1:hms)
out-timendec      =3
out-degform       =deg        # (0:deg,1:dms)
out-outsingle     =on         # (0:off,1:on)
out-maxsolstd     =0.100      # (m) # was 0.005
out-height        =ellipsoidal # (0:ellipsoidal,1:geodetic)
out-geoid         =internal   # (0:internal,1:egm96,2:egm08_2.5,3:egm08_1,4:gsi2000)
out-solstatic     =single     # (0:all,1:single)
out-outstat       =off        # (0:off,1:state,2:residual)
stats-eratio1     =300
stats-eratio2     =300
stats-errphase    =0.003      # (m)
stats-errphaseel  =0.003      # (m)
stats-errphasebl  =0          # (m/10km)
stats-errdoppler  =10         # (Hz)
stats-stdbias     =30         # (m)
stats-stdiono     =0.03       # (m)
stats-stdtrop     =0.3        # (m)
stats-prnaccelh   =10         # (m/s^2)
stats-prnaccelv   =10         # (m/s^2)
stats-prnbias     =0.0001     # (m)
stats-prniono     =0.001      # (m)
stats-prntrop     =0.0001     # (m)
stats-prnpos      =0          # (m)
stats-clkstab     =5e-12      # (s/s)
ant1-postype      =llh        # (0:llh,1:xyz,2:single,3:posfile,4:rinexhead,5:rtcm,6:raw)
ant1-pos1         =90         # (deg|m)
ant1-pos2         =0          # (deg|m)
ant1-pos3         =-6335367.6285 # (m|m)
ant1-anttype      =*
ant1-antdele      =0          # (m)
ant1-antdeln      =0          # (m)
ant1-antdelu      =0          # (m)
ant2-postype      =xyz        # (0:llh,1:xyz,2:single,3:posfile,4:rinexhead,5:rtcm,6:raw)
ant2-pos1         =4399182.9650              # (deg|m)
ant2-pos2         =597294.4500          # (deg|m)
ant2-pos3         =4566748.1240           # (m|m)
ant2-anttype      =*
ant2-initrst      =off        # (0:off,1:on)
misc-timeinterp   =off        # (0:off,1:on)
file-satantfile   =/ifi-NAS/nes/research/gps/external_dataproducts/igs_data/igs08.atx
file-rcvantfile   =/ifi-NAS/nes/research/gps/external_dataproducts/igs_data/igs08.atx
file-ionofile     =/ifi-NAS/nes/research/gps/external_dataproducts/igs_data/igsg%n0.%yi
file-dcbfile      =/ifi-NAS/nes/research/gps/external_dataproducts/code_data/P1P2%y%m.DCB
file-eopfile      =/ifi-NAS/nes/research/gps/external_dataproducts/igs_data/igs%W7.erp
```

Figure B3. The rtkpost options file specifies the processing options - part 2.

https://doi.org/10.5194/essd-2021-176
Preprint. Discussion started: 11 June 2021

Author contributions. JB, AC and SW developed the concept for the manuscript and wrote the bulk of the text. JB, SG, AH, SW, BB AB, MM, RL, TG and RdF developed the sensor technology as well as the data management architecture as well as the tools for managing the data. VW, SG, HR and JB conceived the initial GNSS sensor deployments with the help of LT, TS, AV and DvM that jointly had instrumental roles in launching and executing the initial X-Sense project. PL implemented the first GNSS post-processing prototype. JB, AV, SW, AC, AH, HR, LT, Ts, RD, IGR, RM, JN, MP, EP, CS and DvM contributed to the scaling and application of the technology to further field sites and applications, especially in the domain of long-term monitoring, natural hazard mitigation and early warning. All authors contributed to the article and approved the submitted manuscript.

Acknowledgements. This research has been supported by the funding through Swiss National Science Foundation NCCR-MICS, the ETH Zurich Competence Center on Environment and Sustainability (CCES), the Swiss Federal Office of the Environment (FOEN), nano-tera.ch (grant no. 530659) as well as the Swiss Permafrost Monitoring Network (PERMOS). Support in the form of equipment has been given by Hilti Schweiz AG, Arc'teryx, Petzl and Beal. The technical workshops at ETHZ and UniZH as well as Art of Technology, Zurich, contributed to the successful development and implementation of various pieces of equipment. Furthermore we are thankful for technical support and consultancy by Art of Technology, Zurich, CH (Rolf Schmid) as well as Swisstopo, Wabern, CH (Elmar Brockmann). We are indebted to the extraordinary local support we have received for our research activities in the Matter and Saas Valleys, specifically the municipality of Zermatt (Romy Biner-Hauser), St. Niklaus (Gaby Fux), Herbriggen, Randa, Taesch (Klaus Tscherrig) and Saas Grund, the whole team of Air Zermatt (Gerold Biner), Kurt Lauber, Stephanie Mayor, Martin and Edith Lehner and the Hörnlihütte team, Europahütte (Marcel Brantschen), Kinnhütte (Victor Imboden), Alpin Center Zermatt, Kurt Guntli (Zermatter Bergbahnen), Willy Gitz and Angelo Gruber (Sprengtechnik-GFS), Hotel Bahnhof, Zermatt (Fabi Lauber) as well as the local mountain guides Hermann Biner, Robert Andenmatten, Willy Taugwalder, Urs Lerjen, Benedikt Perren, Bruno Jelk, Hannes Walser, Simon Anthamatten, Yann Dupertuis and Anjan Truffer. Without this strong positive welcome this work would not have been possible. What would we have done without our "homebase" at Hotel Bergfreund in Herbriggen, CH? Big thank you for the generous support to all generations of the whole family Rosi and Rudi Allmendinger. Many friends and helpers were involved in supporting the field work: Lucas Girard, Stephanie Gubler, Christoph Walser, Robert Kenner, Johann Müller, Jeff Moore and Valentin Gischig.

https://doi.org/10.5194/essd-2021-176
Preprint. Discussion started: 11 June 2021

References

Arenson, L., Hoelzle, M., and Springman, S.: Borehole deformation measurements and internal structure of some rock glaciers in Switzerland, Permafrost and Periglacial Processes, 13, 117–135, https://doi.org/https://doi.org/10.1002/ppp.414, https://onlinelibrary.wiley.com/doi/abs/10.1002/ppp.414, 2002.

Arenson, L. U., Kääb, A., and O'Sullivan, A.: Detection and Analysis of Ground Deformation in Permafrost Environments, Permafrost and Periglacial Processes, 27, 339–351, https://doi.org/https://doi.org/10.1002/ppp.1932, https://onlinelibrary.wiley.com/doi/abs/10.1002/ppp.1932, 2016.

Beutel, J., Gruber, S., Hasler, A., Lim, R., Meier, A., Plessl, C., Talzi, I., Thiele, L., Tschudin, C., Woehrle, M., and Yuecel, M.: PermaDAQ: A scientific instrument for precision sensing and data recovery in environmental extremes, in: The 8th ACM/IEEE International Conference on Information Processing in Sensor Networks, pp. 265–276, 2009.

Beutel, J., Buchli, B., Ferrari, F., Keller, M., Thiele, L., and Zimmerling, M.: X-Sense: Sensing in Extreme Environments, Proceedings of Design, Automation and Test in Europe (DATE 2011), pp. 1460–1465, https://doi.org/10.1109/DATE.2011.5763236, 2011.

Biskaborn, B. K., Smith, S. L., Noetzli, J., Matthes, H., Vieira, G., Streletskiy, D. A., Schoeneich, P., Romanovsky, V. E., Lewkowicz, A. G., Abramov, A., Allard, M., Boike, J., Cable, W. L., Christiansen, H. H., Delaloye, R., Diekmann, B., Drozdov, D., Etzelmüller, B., Grosse, G., Guglielmin, M., Ingeman-Nielsen, T., Isaksen, K., Ishikawa, M., Johansson, M., Johannsson, H., Joo, A., Kaverin, D., Kholodov, A., Konstantinov, P., Kröger, T., Lambiel, C., Lanckman, J.-P., Luo, D., Malkova, G., Meiklejohn, I., Moskalenko, N., Oliva, M., Phillips, M., Ramos, M., Sannel, A. B. K., Sergeev, D., Seybold, C., Skryabin, P., Vasiliev, A., Wu, Q., Yoshikawa, K., Zheleznyak, M., and Lantuit, H.: Permafrost is warming at a global scale, Nature Communications, 10, https://doi.org/10.1038/s41467-018-08240-4, 2019.

Bu, J., Yu, K., Qian, N., Zuo, X., and Chang, J.: Performance Assessment of Positioning Based on Multi-Frequency Multi-GNSS Observations: Signal Quality, PPP and Baseline Solution, IEEE Access, 9, 5845–5861, https://doi.org/10.1109/ACCESS.2020.3048352, 2021.

Buchli, B., Sutton, F., and Beutel, J.: GPS-equipped Wireless Sensor Network Node for High-accuracy Positioning Applications, Lecture Notes on Computer Science 7158. Proc. of 9th European Conference on Wireless Sensor Networks (EWSN 2012), pp. 179–195, 2012.

Burjánek, J., Gassner-Stamm, G., Poggi, V., Moore, J. R., and Fäh, D.: Ambient vibration analysis of an unstable mountain slope, Geophysical Journal International, 180, 820–828, https://doi.org/10.1111/j.1365-246X.2009.04451.x, 2010.

Cicoira, A., Beutel, J., Faillettaz, J., Gärtner-Roer, I., and Vieli, A.: Resolving the influence of temperature forcing through heat conduction on rock glacier dynamics: a numerical modelling approach, The Cryosphere, 13, 927–942, https://doi.org/10.5194/tc-13-927-2019, 2019a.

Cicoira, A., Beutel, J., Faillettaz, J., and Vieli, A.: Water controls the seasonal rhythm of rock glacier flow, Earth and Planetary Science Letters, 528, 115 844, https://doi.org/https://doi.org/10.1016/j.epsl.2019.115844, 2019b.

Cicoira, A., Marcer, M., Gärtner-Roer, I., Bodin, X., Arenson, L. U., and Vieli, A.: A general theory of rock glacier creep based on in-situ and remote sensing observations, Permafrost and Periglacial Processes, 32, 139–153, https://doi.org/https://doi.org/10.1002/ppp.2090, 2021.

Dach, R., Lutz, S., Walser, P., and Fridez, P.: Bernese GNSS Software Version 5.2. User manual, Astronomical Institute, University of Bern, https://doi.org/10.7892/boris.72297, 2015.

Delaloye, R., Lambiel, C., and Gärtner-Roer, I.: Overview of rock glacier kinematics research in the Swiss Alps: Seasonal rhythm, interannual variations and trends over several decades, Geogr. Helv., 65, 135–145, https://doi.org/10.5194/gh-65-135-2010, 2010.

Delaloye, R., Morard, S., Barboux, C., Abbet, D., Gruber, V., Riedo, M., and Gachet, S.: Rapidly moving rock glaciers in Mattertal, in: Mattertal – ein Tal in Bewegung, Publikation zur Jahrestagung der Schweizerischen Geomorphologischen Gesellschaft, pp. 21–30, Eidg. Forschungsanstalt WSL, Birmensdorf, CH, St. Niklaus, CH, 2013.

https://doi.org/10.5194/essd-2021-176
Preprint. Discussion started: 11 June 2021

Delaloye, R., Barboux, C., Bodin, X., Brenning, A., Hartl, L., Hu, Y., Ikeda, A., Kaufmann, V., Kellerer-Pirklbauer, A., Lambiel, C., Liu, L., Marcer, M., Rick, B., Scotti, R., Takadema, H., Trombotto Liaudat, D., Vivero, S., and Winterberger, M.: Rock glacier inventories and kinematics: a new IPA Action Group, in: Book of abstracts of the 5th European Conference on Permafrost, pp. 391–392, 2018.

Eberhardt, E., Stead, D., and Coggan, J.: Numerical analysis of initiation and progressive failure in natural rock slopes – The 1991 Randa rockslide, Int. J. Rock Mech. Min., 41, 69–87, https://doi.org/10.1016/S1365-1609(03)00076-5, 2004.

Fäh, D., Moore, J., Burjanek, J., Iosifescu Enescu, I., Dalguer, L., Dupray, F., Michel, C., Woessner, J., Villiger, A., Laue, J., Marschall, I., Gischig, V., Loew, S., Alvarez, S., Balderer, W., Kästli, P., Giardini, D., Iosifescu Enescu, C. M., Hurni, L., Lestuzzi, P., Karbassi, A., Baumann, C., Geiger, A., Ferrari, A., Lalou, L., Clinton, J., and Deichmann, N.: Coupled seismogenic geohazards in alpine regions, Bollettino di Geofisica Teorica ed Applicata, 53, 485 – 508, https://doi.org/10.4430/bgta0048, 2012-12.

Girard, L., Beutel, J., Gruber, S., Hunziker, J., Lim, R., and Weber, S.: A custom acoustic emission monitoring system for harsh environments: Application to freezing-induced damage in alpine rock walls, Geosci. Instrum. Method. Data Syst., 1, 155–167, https://doi.org/10.5194/gi-1-155-2012, 2012.

Gischig, S., Moore, J. R., Evans, K. F., Amann, F., and Loew, S.: Thermomechanical forcing of deep rock slope deformation: 2. The Randa rock slope instability, Journal of Geophysical Research: Earth Surface, 116, https://doi.org/10.1029/2011JF002007, 2011a.

Gischig, V., Amann, F., Moore, J., Loew, S., Eisenbeiss, H., and Stempfhuber, W.: Composite rock slope kinematics at the current Randa instability, Switzerland, based on remote sensing and numerical modeling, Engineering Geology, 118, 37–53, https://doi.org/https://doi.org/10.1016/j.enggeo.2010.11.006, https://www.sciencedirect.com/science/article/pii/S0013795210002371, 2011b.

Guillemot, A., Baillet, L., Garambois, S., Bodin, X., Helmstetter, A., Mayoraz, R., and Larose, E.: Modal sensitivity of rock glaciers to elastic changes from spectral seismic noise monitoring and modeling, The Cryosphere, 15, 501–529, https://doi.org/10.5194/tc-15-501-2021, https://tc.copernicus.org/articles/15/501/2021/, 2021.

Haeberli, W.: Creep of mountain permafrost: Internal Structure and Flow of Alpine Rock Glaciers, Ph.D. thesis, ETH Zurich, 1985.

Haeberli, W.: On the morphodynamics of ice/ debris-transport systems in cold mountain areas, Norsk Geografisk Tidsskrift, 50, 3–9, https://doi.org/10.1080/00291959608552346, 1996.

Haeberli, W. and Schmid, W.: Aerophotogrammetrical monitoring of rock glaciers, in: Proc. Fifth International Conference on Permafrost, pp. 764–769, International Permafrost Association, Trondheim, Norway, 1988.

Haeberli, W. and Vonder Mühll, D.: On the characteristics and possible origins of ice in rock glacier permafrost, Zeitschrift fur Geomorphologie, pp. 43–57, 1996.

Haeberli, W., King, L., and Flotron, A.: Surface movement and lichen-cover studies at the active rock glacier near the Grubengletscher, Wallis, Swiss Alps, Arctic and Alpine Research, 11, 421–441, 1979.

Hasler, A., Talzi, I., Beutel, J., Tschudin, C., and Gruber, S.: Wireless sensor networks in permafrost research: Concept, requirements, implementation, and challenges, in: Proceedings of the 9th International Conference on Permafrost, 2008.

Hasler, A., Gruber, S., and Haeberli, W.: Temperature variability and offset in steep alpine rock and ice faces, The Cryosphere, 5, 977–988, https://doi.org/10.5194/tc-5-977-2011, 2011.

Hasler, A., Gruber, S., and Beutel, J.: Kinematics of steep bedrock permafrost, J. Geophys. Res., 117, F01 016, https://doi.org/10.1029/2011JF001981, 2012.

https://doi.org/10.5194/essd-2021-176
Preprint. Discussion started: 11 June 2021

Henkel, P., Koch, F., Appel, F., Bach, H., Prasch, M., Schmid, L., Schweizer, J., and Mauser, W.: Snow Water Equivalent of Dry Snow Derived From GNSS Carrier Phases, IEEE Transactions on Geoscience and Remote Sensing, 56, 3561–3572, https://doi.org/10.1109/TGRS.2018.2802494, 2018.

Hoelzle, M., Vonder Mühll, D., and Haeberli, W.: Thirty years of permafrost research in the Corvatsch-Furtschellas area, Eastern Swiss Alps: A review, Norsk Geografisk Tidsskrift - Norwegian Journal of Geography, 56, 137–145, https://doi.org/10.1080/002919502760056468, 2002.

Hurter, F., Geiger, A., Perler, D., and Rothacher, M.: GNSS water vapor monitoring in the Swiss Alps, in: 2012 IEEE International Geoscience and Remote Sensing Symposium, pp. 1972–1975, https://doi.org/10.1109/IGARSS.2012.6351115, 2012.

Kääb, A., Jacquemart, M., Gilbert, A., Leinss, S., Girod, L., Huggel, C., Falaschi, D., Ugalde, F., Petrakov, D., Chernomorets, S., Dokukin, M., Paul, F., Gascoin, S., Berthier, E., and Kargel, J. S.: Sudden large-volume detachments of low-angle mountain glaciers – more frequent than thought?, The Cryosphere, 15, 1751–1785, https://doi.org/10.5194/tc-15-1751-2021, https://tc.copernicus.org/articles/15/1751/2021/, 2021.

Kaeaeb, A., Gudmundsson, G. H., and Hoelzle, M.: Surface deformation of creeping mountain permafrost. Photogrammetric investigations on Murtel Rock Glacier, Swiss Alps, in: Proc. Seventh International Conference on Permafrost, pp. 531–537, International Permafrost Association, Yellowknife, Canada, 1998.

Kenner, R., Phillips, M., Beutel, J., Hiller, M., Limpach, P., Pointner, E., and Volken, M.: Factors Controlling Velocity Variations at Short-Term, Seasonal and Multiyear Time Scales, Ritigraben Rock Glacier, Western Swiss Alps, Permafrost and Periglacial Processes, 28, 675–684, https://doi.org/10.1002/ppp.1953, 2017.

Kenner, R., Phillips, M., Limpach, P., Beutel, J., and Hiller, M.: Monitoring mass movements using georeferenced time-lapse photography: Ritigraben rock glacier, western Swiss Alps, Cold Regions Science and Technology, 145, 127 – 134, https://doi.org/https://doi.org/10.1016/j.coldregions.2017.10.018, 2018.

Kenner, R., Pruessner, L., Beutel, J., Limpach, P., and Phillips, M.: How rock glacier hydrology, deformation velocities and ground temperatures interact: Examples from the Swiss Alps, Permafrost and Periglacial Processes, 31, 3–14, https://doi.org/10.1002/ppp.2023, 2020.

Kummert, M. and Delaloye, R.: Mapping and quantifying sediment transfer between the front of rapidly moving rock glaciers and torrential gullies, Geomorphology, 309, 60–76, https://doi.org/https://doi.org/10.1016/j.geomorph.2018.02.021, https://www.sciencedirect.com/science/article/pii/S0169555X18300795, 2018.

Kummert, M., Delaloye, R., and Braillard, L.: Erosion and sediment transfer processes at the front of rapidly moving rock glaciers: Systematic observations with automatic cameras in the western Swiss Alps, Permafrost and Periglacial Processes, 29, 21–33, https://doi.org/https://doi.org/10.1002/ppp.1960, https://onlinelibrary.wiley.com/doi/abs/10.1002/ppp.1960, 2018a.

Kummert, M., Delaloye, R., and Braillard, L.: Erosion and sediment transfer processes at the front of rapidly moving rock glaciers: Systematic observations with automatic cameras in the western Swiss Alps, Permafrost and Periglacial Processes, 29, 21–33, https://doi.org/https://doi.org/10.1002/ppp.1960, https://onlinelibrary.wiley.com/doi/abs/10.1002/ppp.1960, 2018b.

Kääb, A., Haeberli, W., and Gudmundsson, G. H.: Analysing the creep of mountain permafrost using high precision aerial photogrammetry: 25 years of monitoring Gruben rock glacier, Swiss Alps, Permafrost and Periglacial Processes, 8, 409–426, https://doi.org/https://doi.org/10.1002/(SICI)1099-1530(199710/12)8:4<409::AID-PPP267>3.0.CO;2-C, 1997.

Lambiel, C. and Delaloye, R.: Contribution of real-time kinematic GPS in the study of creeping mountain permafrost: examples from the Western Swiss Alps, Permafrost and Periglacial Processes, 15, 229–241, https://doi.org/https://doi.org/10.1002/ppp.496, https://onlinelibrary.wiley.com/doi/abs/10.1002/ppp.496, 2004.

https://doi.org/10.5194/essd-2021-176
Preprint. Discussion started: 11 June 2021

Marcer, M., Cicoira, A., Cusicanqui, D., Bodin, X., Echelard, T., Obregon, R., , and Schoeneich, P.: Rock glaciers throughout the French Alps accelerated and destabilised since 1990 as air temperatures increased, Communications Earth and Environment, 2, https://doi.org/https://doi.org/10.1038/s43247-021-00150-6, 2021.

Moore, J., Gischig, V., Burjánek, J., Loew, S., , and Fäh, D.: Site effects in unstable rock slopes: Dynamic behavior of the Randa instability (Switzerland), Bull. Seism. Soc. Am., 101, 3110–3116, https://doi.org/10.1785/0120110127, 2011.

Noetzli, J., Pellet, C., and Staub, B., eds.: PERMOS 2019. Permafrost in Switzerland 2014/2015 to 2017/2018, Glaciological Report (Permafrost) No. 16-19 of the Cryospheric Commission of the Swiss Academy of Sciences (SCNAT), https://doi.org/10.13093/permos-rep-2019-16-19, 2019.

Oggier, N., Graf, C., Delaloye, R., and Burkard, A.: Integral protection concept "Bielzug" - Integrales Schutzkonzept Bielzug, in: Proc. INTERPRAEVENT 2016, pp. 525–534, 2016.

Paziewski, J., Fortunato, M., Mazzoni, A., and Odolinski, R.: An analysis of multi-GNSS observations tracked by recent Android smartphones and smartphone-only relative positioning results, Measurement, 175, 109 162, https://doi.org/https://doi.org/10.1016/j.measurement.2021.109162, https://www.sciencedirect.com/science/article/pii/S0263224121001858, 2021.

Ravanel, L. and Deline, P.: Rockfall hazard in the Mont Blanc massif increased by the current atmospheric warming, in: IAEG 12th Congress, edited by Lollino, G., Manconi, A., Clague, J., Shan, W., and Chiarle, M., Climate Change and Engineering Geology, pp. p. 425–428, Torino, Italy, https://hal-sde.archives-ouvertes.fr/hal-01896005, 2014.

Scapozza, C., Lambiel, C., Bozzini, C., Mari, S., and Conedera, M.: Assessing the rock glacier kinematics on three different timescales: a case study from the southern Swiss Alps, Earth Surface Processes and Landforms, 39, 2056–2069, https://doi.org/https://doi.org/10.1002/esp.3599, https://onlinelibrary.wiley.com/doi/abs/10.1002/esp.3599, 2014.

Strozzi, T., Caduff, R., Jones, N., Barboux, C., Delaloye, R., Bodin, X., Kääb, A., Mätzler, E., and Schrott, L.: Monitoring Rock Glacier Kinematics with Satellite Synthetic Aperture Radar, Remote Sensing, 12, https://doi.org/10.3390/rs12030559, https://www.mdpi.com/2072-4292/12/3/559, 2020.

Talzi, I., Hasler, A., Gruber, S., and Tschudin, C.: PermaSense: Investigating Permafrost with a WSN in the Swiss Alps, in: Proceedings of the 4th Workshop on Embedded Networked Sensors, EmNets '07, pp. 8–12, ACM, New York, NY, USA, https://doi.org/10.1145/1278972.1278974, 2007.

Teunissen, P. J. and Montenbruck, O., eds.: Handbook of Global Navigation Satellite Systems, Springer International Publishing, https://doi.org/10.1007/978-3-319-42928-1, 2017.

Vonder Mühll, D. and Haeberli, W.: Thermal Characteristics of the Permafrost within an Active Rock Glacier (Murtèl/Corvatsch, Grisons, Swiss Alps), Journal of Glaciology, 36, 151–158, https://doi.org/10.3189/S0022143000009382, 1990.

Weber, S., Beutel, J., Faillettaz, J., Hasler, A., Krautblatter, M., and Vieli, A.: Quantifying irreversible movement in steep, fractured bedrock permafrost on Matterhorn (CH), The Cryosphere, 11, 567–583, https://doi.org/10.5194/tc-11-567-2017, 2017.

Weber, S., Beutel, J., Gruber, S., Gsell, T., Hasler, A., and Vieli, A.: Rock-temperature, fracture displacement and acoustic/micro-seismic data measured at Matterhorn Hörnligrat, Switzerland, https://doi.org/10.5281/zenodo.1163037, 2018a.

Weber, S., Fäh, D., Beutel, J., Faillettaz, J., Gruber, S., and Vieli, A.: Ambient seismic vibrations in steep bedrock permafrost used to infer variations of ice-fill in fractures, Earth and Planetary Science Letters, 501, 119–127, https://doi.org/10.1016/j.epsl.2018.08.042, 2018b.

Weber, S., Faillettaz, J., Meyer, M., Beutel, J., and Vieli, A.: Acoustic and micro-seismic characterization in steep bedrock permafrost on Matterhorn (CH), Journal of Geophysical Research: Earth Surface, 123, 1363–1385, https://doi.org/10.1029/2018JF004615, 2018c.

https://doi.org/10.5194/essd-2021-176
Preprint. Discussion started: 11 June 2021

Weber, S., Beutel, J., Da Forno, R., Geiger, A., Gruber, S., Gsell, T., Hasler, A., Keller, M., Lim, R., Limpach, P., Meyer, M., Talzi, I., Thiele, L., Tschudin, C., Vieli, A., Vonder Mühll, D., and Yücel, M.: A decade of detailed observations (2008–2018) in steep bedrock permafrost at Matterhorn Hörnligrat (Zermatt, CH), Earth System Science Data, 2019, 1203–1237, https://doi.org/10.5194/essd-11-1203-2019, 2019a.

Weber, S., Beutel, J., and Meyer, M.: Code for PermaSense GSN data management, https://doi.org/10.5281/zenodo.2542714, 2019b.

Willenberg, H., Evans, K. F., Eberhardt, E., Spillmann, T., and Loew, S.: Internal structure and deformation of an unstable crystalline rock mass above Randa (Switzerland): Part II — Three-dimensional deformation patterns, Engineering Geology, 101, 15–32, https://doi.org/https://doi.org/10.1016/j.enggeo.2008.01.016, https://www.sciencedirect.com/science/article/pii/S0013795208000264, 2008a.

Willenberg, H., Loew, S., Eberhardt, E., Evans, K. F., Spillmann, T., Heincke, B., Maurer, H., and Green, A. G.: Internal structure and deformation of an unstable crystalline rock mass above Randa (Switzerland): Part I — Internal structure from integrated geological and geophysical investigations, Engineering Geology, 101, 1–14, https://doi.org/https://doi.org/10.1016/j.enggeo.2008.01.015, https://www.sciencedirect.com/science/article/pii/S0013795208000239, 2008b.

Wirz, V., Beutel, J., Buchli, B., Gruber, S., and Limpach, P.: Temporal Characteristics of Different Cryosphere-Related Slope Movements in High Mountains, pp. 383–390, Springer, Berlin, Heidelberg, https://doi.org/10.1007/978-3-642-31337-0_49, 2013.

Wirz, V., Beutel, J., Gruber, S., Gubler, S., and Purves, R. S.: Estimating velocity from noisy GPS data for investigating the temporal variability of slope movements, Natural Hazards and Earth System Sciences, 14, 2503–2520, https://doi.org/10.5194/nhess-14-2503-2014, 2014a.

Wirz, V., Geertsema, M., Gruber, S., and Purves, R. S.: Temporal variability of diverse mountain permafrost slope movements derived from multi-year daily GPS data, Mattertal, Switzerland, Landslides, 13, 67–83, https://doi.org/10.1007/s10346-014-0544-3, 2014b.

Wirz, V., Gruber, S., Purves, R. S., Beutel, J., Gärtner-Roer, I., Gubler, S., and Vieli, A.: Short-term velocity variations at three rock glaciers and their relationship with meteorological conditions, Earth Surf. Dynam., 4, 103–123, https://doi.org/10.5194/esurf-4-103-2016, 2016.